AMERICAN SOCIETY FOR MICROBIOLOGY | Infection and Immunity®

MOLECULAR PATHOGENESIS

Immediate Interferon Gamma Induction Determines Murine Host Compatibility Differences between *Toxoplasma gondii* and *Neospora caninum*

Rachel S. Coombs,[a] Matthew L. Blank,[a] Elizabeth D. English,[a] Yaw Adomako-Ankomah,[a] Ifeanyi-Chukwu Samuel Urama,[a] Andrew T. Martin,[b] Felix Yarovinsky,[b] Jon P. Boyle[a]

[a]Department of Biological Sciences, University of Pittsburgh, Pittsburgh, Pennsylvania, USA
[b]Center for Vaccine Biology and Immunology, Department of Microbiology and Immunology, University of Rochester, Rochester, New York, USA

ABSTRACT Rodents are critical for the transmission of *Toxoplasma gondii* to the definitive feline host via predation, and this relationship has been extensively studied as a model for immune responses to parasites. *Neospora caninum* is a closely related coccidian parasite of ruminants and canines but is not naturally transmitted by rodents. We compared mouse innate immune responses to *N. caninum* and *T. gondii* and found marked differences in cytokine levels and parasite growth kinetics during the first 24 h postinfection (hpi). *N. caninum*-infected mice produced significantly higher levels of interleukin-12 (IL-12) and interferon gamma (IFN-γ) by as early as 4 hpi, but the level of IFN-γ was significantly lower or undetectable in *T. gondii*-infected mice during the first 24 hpi. "Immediate" IFN-γ and IL-12p40 production was not detected in MyD88$^{-/-}$ mice. However, unlike IL-12p40$^{-/-}$ and IFN-γ$^{-/-}$ mice, MyD88$^{-/-}$ mice survived *N. caninum* infections at the dose used in this study. Serial measures of parasite burden showed that MyD88$^{-/-}$ mice were more susceptible to *N. caninum* infections than wild-type (WT) mice, and control of parasite burdens correlated with a pulse of serum IFN-γ at 3 to 4 days postinfection in the absence of detectable IL-12. Immediate IFN-γ was partially dependent on the *T. gondii* mouse profilin receptor Toll-like receptor 11 (TLR11), but the ectopic expression of *N. caninum* profilin in *T. gondii* had no impact on early IFN-γ production or parasite proliferation. Our data indicate that *T. gondii* is capable of evading host detection during the first hours after infection, while *N. caninum* is not, and this is likely due to the early MyD88-dependent recognition of ligands other than profilin.

KEYWORDS IL-12, interferon gamma, MyD88, profilin, TLR11, *Toxoplasma gondii*, host response, host-pathogen interactions, innate immunity, *Neospora caninum*

Most parasite species exhibit selective host ranges and infect only one or a small number of intermediate hosts. There are few examples of molecular host range determinants in eukaryotic pathogens, but they are critical for our understanding of the barriers that prevent host jumping or host range expansion. *Toxoplasma gondii* and *Neospora caninum* are parasites with extensive similarity at the genetic level but with markedly distinct abilities to infect rodents in the wild and in the laboratory (1, 2). The mechanisms that determine this difference in host range are unknown. Here, we show that *N. caninum* infection is rapidly controlled in mice, while *T. gondii* infection is not, due to the robust and rapid induction of protective host cytokines. These data suggest that the host range differences between *T. gondii* and *N. caninum* are due to previously unrecognized mechanisms of immediate recognition of *N. caninum* and avoidance or suppression of this response by *T. gondii*.

In contrast to many viruses and a few bacterial pathogens, very little is known about

Citation Coombs RS, Blank ML, English ED, Adomako-Ankomah Y, Urama I-CS, Martin AT, Yarovinsky F, Boyle JP. 2020. Immediate interferon gamma induction determines murine host compatibility differences between *Toxoplasma gondii* and *Neospora caninum*. Infect Immun 88:e00027-20. https://doi.org/10.1128/IAI.00027-20.

Editor Jeroen P. J. Saeij, UC Davis School of Veterinary Medicine

Address correspondence to Jon P. Boyle, boylej@pitt.edu.

Received 13 January 2020
Accepted 13 January 2020
Accepted manuscript posted online 3 February 2020
Published 23 March 2020

the molecular biology of host-pathogen compatibility in eukaryotic parasites, including *Toxoplasma gondii*. Apicomplexan parasites are formidable eukaryotic pathogens responsible for diseases including malaria, cryptosporidiosis, neosporosis, and toxoplasmosis, which kill millions of people and animals worldwide each year (3, 5, 6). Among these important intracellular pathogens, *Toxoplasma gondii* is the only species capable of infecting, causing disease in, and being transmitted by every warm-blooded animal tested to date (7–9). *N. caninum* is the causative agent of neosporosis, a disease that causes fetal death and neonatal mortality (10) in bovine (11), ovine (12), and canine (13) hosts. *N. caninum* is remarkably similar in morphology and genomic synteny (85%) to *T. gondii* (6, 14, 15), but there are important differences in their disease pathologies. Virulent strains of *T. gondii* are known to cause disease worldwide in all animals (8, 9), but *N. caninum* is restricted by a comparatively smaller host range. *N. caninum* causes disease in a limited number of closely related ruminant or canine hosts (11, 16), although *N. caninum* is far more successful in cattle, which are considered poor hosts for *T. gondii* (17–19). Mice are an important natural host for *T. gondii*; infections have been well documented in the laboratory and in nature (20–24), and mice infected with even 1 tachyzoite of virulent *T. gondii* strains will become morbid (25–27). Alternatively, mice infected with up to 1 million tachyzoites of *N. caninum* strains do not exhibit any observable morbidity (1, 28, 29). A large body of work has shown that in mice, proinflammatory responses are the only effective immune response to *N. caninum*, and control is dependent on cytokine production (30–32). Interferon gamma (IFN-γ) has been identified as an important immune-modulating cytokine in mice and cattle during *N. caninum* infections (31, 33), and investigations in both mice and cattle show that the production of IFN-γ is an important protective mechanism during neosporosis (32, 34). While IFN-γ can protect against abortion in cattle, high levels of IFN-γ at the maternofetal interface increase fetal death (35, 36). IFN-γ is required for the acute control of *T. gondii* and is dependent on IFN-γ-driven, cell-mediated immune (CMI) responses where the production of IFN-γ is primarily derived from interleukin-12 (IL-12)-stimulated natural killer (NK) cells and T lymphocytes (37). IFN-γ is also required for resistance to *N. caninum* in mice (38), but the precise mechanisms of resistance and when this cytokine is most critical for resistance are not known.

Our previous work identified a dramatic difference in infection outcomes in BALB/c mice between an avirulent *T. gondii* strain, Tg:S1T:Luc:DsRed (TgS1T:Luc) (generated from a cross between a type II and a type III *T. gondii* strain [39]) and *N. caninum* Nc1:Luc (1). After infection with 10^6 tachyzoites, the parasite-derived luciferase (Luc) signal increased similarly between strains during the first 24 h postinfection (hpi), followed by a rapid decrease of the *N. caninum* bioluminescence signal, while the *T. gondii* signal continued to increase (1). The immediate control of *N. caninum* parasite proliferation *in vivo* was previously unappreciated despite previous work demonstrating a decrease of the *N. caninum*-derived bioluminescence signal at between 1 and 2 days postinfection (dpi) (2) and the extensive use of a mouse model to develop vaccines and treatment for bovine neosporosis (40, 41). The mechanism(s) underlying the dramatic difference between *T. gondii* and *N. caninum* growth during acute infection is unknown. Here, we compare host innate immune responses and parasite proliferation kinetics *in vivo* to identify differences in the host responses to *N. caninum* and *T. gondii* during the first 24 hpi that determine this dramatic difference in infection outcomes.

RESULTS

The mouse host response controls *N. caninum* proliferation within 24 h postinfection. *In vivo* bioluminescence imaging (BLI) is a powerful tool to detect differences in pathogen burdens during live infections in mice (26, 42, 43). The parasite burden correlates directly with photon flux and is calculated by quantifying photonic emission after luciferase substrate injection in live animals (44). By employing this noninvasive technique, we were able to compare the kinetics of *T. gondii* and *N. caninum* proliferation within a single mouse over the course of the infection. First, we selected *T. gondii* strains with well-characterized differences in virulence, selecting high (TgS23:Luc)- and

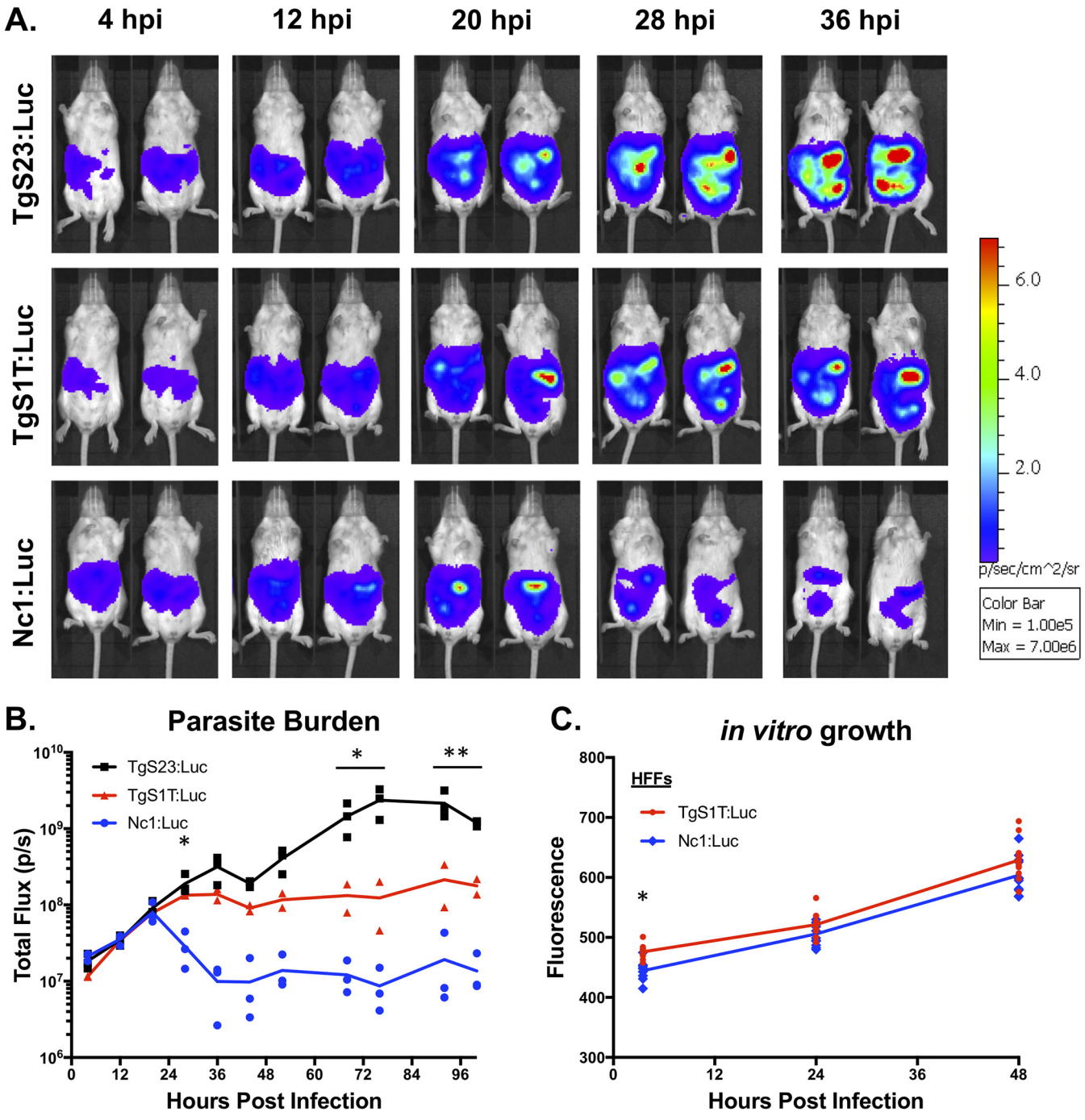

FIG 1 *T. gondii* and *N. caninum* growth rates *in vitro* and *in vivo*. (A) *In vivo* bioluminescence imaging of mice infected with 10^6 parasites of luciferase-expressing *T. gondii* strain TgS1T:Luc or TgS23:Luc or *N. caninum* strain Nc1:Luc. Images were taken every 8 h, starting at 4 h postinfection (hpi). (B) Quantification of images, where each data point represents the total flux (photons per second [p/s]) of an infected mouse (TgS1T:Luc, $n = 2$; TgS23:Luc, $n = 3$; Nc1:Luc, $n = 3$). (C) *In vitro* growth assay of TgS1T:Luc:DsRed (TgS1T:Luc) and Nc1:Luc:DsRed (Nc1:Luc). Human foreskin fibroblasts (HFFs) were inoculated with 10^4 parasites/well in 96-well plates, and fluorescence was measured at the indicated time points. Imaging data were log transformed, and both *in vitro* and *in vivo* assays were analyzed using two-way repeated-measures ANOVA (alpha value of 0.05) with Sidak's multiple-comparison test. *, $P < 0.05$; **, $P < 0.01$.

low (TgS1T:Luc)-virulence *T. gondii* strains for comparison with the *N. caninum* strain Nc1:Luc (26). We selected these F1 progeny for our comparisons because S23 has the "virulent allele" for 5 genes known to impact disease outcome and mortality in mice, while S1T has the "avirulent allele" at these same 5 loci (39, 45). To compare these strains directly, we infected mice intraperitoneally (i.p.) with 10^6 luciferase-expressing tachyzoites and performed *in vivo* BLI (Fig. 1A). Quantification of bioluminescence

images (Fig. 1B) showed that both *T. gondii* strains and *N. caninum* grew at similar rates during the first 20 hpi, after which both *T. gondii* strains continued to proliferate and *N. caninum* was controlled. We observed no statistically significant differences in parasite burdens in the first 20 h comparing all 3 infections (Fig. 1B). We observed statistically significant differences in parasite burdens between TgS1T:Luc and TgS23:Luc, with the latter, more virulent *T. gondii* strain having a higher parasite burden than the TgS1T:Luc strain by 72 hpi (Fig. 1B). Our results were replicated in a second experiment, again using 3 mice per group (data not shown), and are consistent with known virulence differences between the *T. gondii* strains (39) as well as *N. caninum* (46). This suggested that *N. caninum* is limited in its capacity to establish infections in mice after the first 20 h, even compared to the less virulent *T. gondii* strain (TgS1T) (26, 47, 48). To confirm that *N. caninum* parasite growth is controlled within the first 24 h of infection, we performed 3 additional experiments comparing TgS1T:Luc and Nc1:Luc BLI during acute infection (Fig. 2A [TgS1T:Luc, $n = 2$; Nc1:Luc, $n = 3$] and data not shown [$n = 3$ per parasite species]; see also Fig. S1 in the supplemental material [$n = 3$ per parasite species]). The *N. caninum* parasite burden was significantly lower than the *T. gondii* burden ($P < 0.001$) during days 3 to 6 postinfection (p.i.) (Fig. 2A), demonstrating the reproducibility of this observation. Together, these results demonstrate that the *N. caninum*-derived luciferase signal peaks at 24 hpi and therefore appears to be rapidly controlled, while *T. gondii* continues to proliferate for up to 6 to 8 dpi. Importantly, when we compared *in vitro* growth rates of avirulent TgS1T:Luc and Nc1:Luc strains in human foreskin fibroblasts (HFFs), we found no significant differences in parasite-derived fluorescence at 24 or 48 hpi (Fig. 1C).

***N. caninum* infections in mice induce significantly higher levels of proinflammatory cytokines within the first 24 h of infection than do *T. gondii* infections.** Given the clear differences in proliferation *in vivo* between *N. caninum* and *T. gondii* (Fig. 1A and B), we hypothesized that the host innate response might be responsible for the observed *in vivo* proliferation differences. To test this hypothesis, we performed an initial screen using a Luminex multiplex assay to compare the levels of 32 mouse chemokines and cytokines by comparing analyte fluorescence in *T. gondii* to that in *N. caninum* infections. Mice ($n = 3$ per species) were infected i.p. with 10^6 tachyzoites of either TgS1T:Luc or Nc1:Luc, and serum or peritoneal lavage samples were collected at 14 hpi and screened for analyte differences between parasite species (Fig. S2A and B). These comparisons revealed that *N. caninum* infection induced a distinct cytokine/chemokine profile very early after infection compared to that of *T. gondii*, including several critical inflammatory cytokines known to be important for controlling intracellular parasite infections. Of note, we observed large (>10-fold) differences in serum IFN-γ, IL-12p70, IL-12p40, and CCL2 (monocyte chemoattractant protein [MCP]) levels compared to those in *T. gondii*-infected mice, while other queried cytokines, such as IP-10 (interferon gamma-inducible protein 10, or CXCL10) and MIG (monokine induced by gamma, or CXCL9), were either poorly induced or induced similarly by both species (Fig. S2A and B). Next, we wanted to screen additional time points to see how early these changes were detectable in our cytokine panel, so we tested 2 mice per parasite species at the time point of 4 or 8 hpi and analyzed serum with the same Luminex panel. We observed similar differential production of cytokines at both 4 and 8 hpi comparing *T. gondii* and *N. caninum* (Fig. S2C and D). This screen suggested that IL-12 and IFN-γ production occurred in response to *N. caninum* infection by as early as 4 hpi, while the levels of these cytokines were lower or undetectable at these time points in *T. gondii*-infected mice (Fig. S2).

To confirm these results, we infected 3 BALB/c mice per group with 10^6 Nc1:Luc or TgS1T:Luc tachyzoites, collected serum, and measured IL-12p40 and IFN-γ levels at multiple time points in the first 24 h of infection by an enzyme-linked immunosorbent assay (ELISA). In *N. caninum*-infected mice, we detected serum IL-12p40 (Fig. 2B) and IFN-γ (Fig. 2C) by as early as 4 hpi, while we detected significantly less serum IL-12p40 ($P < 0.001$) (Fig. 2B) and detected no IFN-γ (Fig. 2C) in *T. gondii*-infected mice during the first 24 hpi. To confirm that TgS1T:Luc-infected mice did not induce early IFN-γ, the

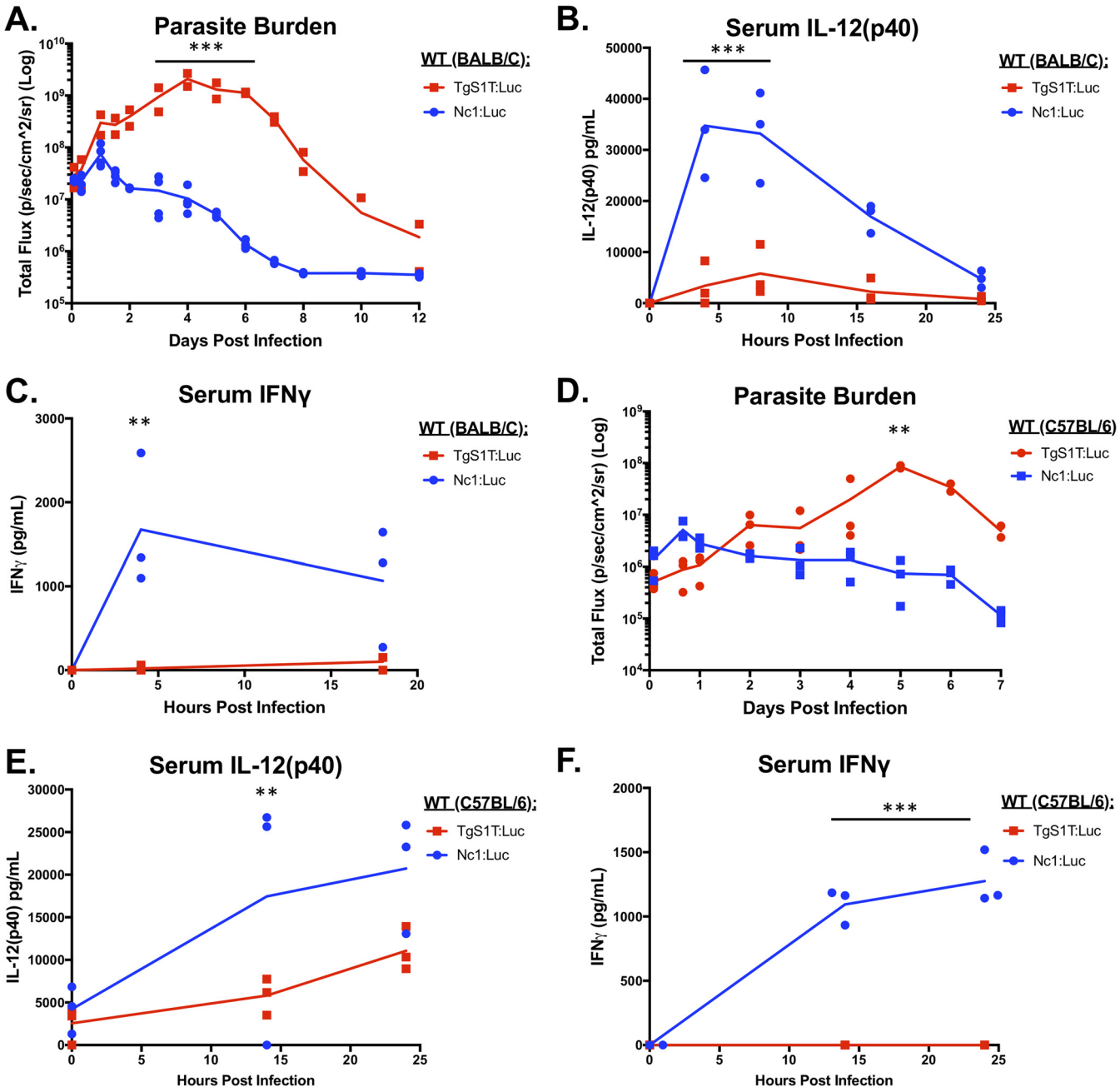

FIG 2 Parasite burden and day 0 to 1 cytokine levels in mice infected with *N. caninum* (Nc1) or *T. gondii* (S1T). Six-week-old BALB/c (A to C) or C57BL/6 (D to F) mice were i.p. injected with 10^6 TgS1T:Luc or Nc1:Luc tachyzoites. Bioluminescence imaging was used to monitor the parasite burden over the course of the infection. Serum was collected and analyzed for IL-12p40 or IFN-γ by an ELISA. (A) Quantification of bioluminescence during *in vivo* infections in BALB/c mice (TgS1T:Luc, $n = 2$; Nc1:Luc, $n = 3$) (the experiment was repeated [see Fig. S1 in the supplemental material]). (B and C) Cytokine quantification using an ELISA for mouse IL-12p40 (B) or IFN-γ (C) ($n = 3$ per parasite species). (D to F) Same as panels A to C but with C57BL/6 mice ($n = 3$ per species; this experiment was performed only once). For all experiments, imaging data were log transformed, and two-way repeated-measures ANOVA (alpha value of 0.05) with Sidak's multiple-comparison test was then performed. Cytokines were analyzed by two-way repeated-measures ANOVA (alpha value of 0.05) with Sidak's multiple-comparison test. **, $P < 0.01$; ***, $P < 0.001$.

experiment was repeated twice, with similar results (Fig. S1B [$n = 3$ per parasite species] and data not shown [$n = 3$ per parasite species]).

To ensure that this growth and cytokine response phenotype was not specific to BALB/c mice, we also compared *T. gondii* and *N. caninum* infections in C57BL/6 mice ($n = 3$ per parasite species) (Fig. 2D). We observed that, similar to BALB/c infections, C57BL/6 mice controlled *N. caninum* infections within 24 hpi, and the *N. caninum*

burden was significantly lower at 5 dpi in C57BL/6 mice. This confirms the findings of others that BALB/c and C57BL/6 mice have similar susceptibilities to *N. caninum* infection (29, 31, 49). We also observed cytokine profiles in C57BL/6 mice that were similar to those observed in BALB/c mice. Specifically, we detected significantly higher levels of IL-12p40 (Fig. 2E) and IFN-γ (Fig. 2F) during the first 24 h of *N. caninum* infections than for *T. gondii* infections ($P < 0.01$; $P < 0.001$), and, as for BALB/c mice, IFN-γ was not detectable in *T. gondii*-infected mouse sera in the first 24 h of infection (Fig. 2F). Thus, using two different detection methods (ELISA and Luminex), we observed consistent differences in cytokine production in *N. caninum* infections in either mouse strain tested.

IFN-γ is required for control of *N. caninum* proliferation. IFN-γ is a critical cytokine for both innate and adaptive immunity and is required for the acute control of *T. gondii* infections in mice (38). Previous work has shown that mice deficient in IFN-γ (both IFN-γ depleted and IFN-$\gamma^{-/-}$) are also susceptible to *N. caninum* parasites (32, 50), but the impact of IFN-γ deletion on parasite kinetics during *N. caninum* infection is unknown. To quantify this, we injected 10^6 tachyzoites of either TgS1T:Luc or Nc1:Luc intraperitoneally into either IFN-$\gamma^{-/-}$ or wild-type (WT) mice ($n = 3$ per mouse strain and parasite species), calculated the parasite burden using BLI (Fig. 3A and C), and monitored mouse survival (Fig. 3B). As expected, mice lacking IFN-γ succumbed to *N. caninum* infection in a similar time frame as those infected with *T. gondii* (Fig. 3B). Surprisingly, we found that the *N. caninum* parasite burden significantly exceeded that of *T. gondii* at days 4 and 5 postinfection in IFN-$\gamma^{-/-}$ mice (Fig. 3C) despite exhibiting similar levels of burden and proliferation in the first 24 h (Fig. 3C, inset). These results were confirmed by an additional experiment ($n = 3$ per mouse strain and parasite species) (Fig. 3B and Fig. S3A) showing that IFN-γ knockout mice are more susceptible to *N. caninum* than they are to *T. gondii*.

One reason for the dramatic differences in parasite control during the first 24 hpi could be due to differences in susceptibility to IFN-γ-induced parasiticidal mediators between *T. gondii* and *N. caninum*. To compare IFN-γ susceptibilities, we performed *in vitro* growth assays in mouse embryonic fibroblasts (MEFs) in the presence or absence of IFN-γ. MEF monolayers in 96-well plates were infected with 10^4 tachyzoites of either TgS1T:Luc or Nc1:Luc for 24 h and then treated with either 100 U/ml or 0 U/ml of recombinant mouse IFN-γ (Fig. 3D). We quantified parasite numbers by measuring total DsRed-derived fluorescence (as both Nc1:Luc and S1T:Luc also expressed DsRed from the same promoter [see Materials and Methods]). We did not find any evidence for higher IFN-γ susceptibly in *N. caninum* than in *T. gondii* (Fig. 3D), in that both parasite species had similar growth profiles in the presence of mouse IFN-γ. These results were confirmed in one additional experiment (data not shown). These data suggest that differences in *in vivo* proliferation between *T. gondii* and *N. caninum* in WT and IFN-$\gamma^{-/-}$ mice are unlikely to be due to differences in IFN-γ susceptibility.

IL-12p40 is less critical for host resistance to *N. caninum* than IFN-γ. Previous work has shown that IL-12p40$^{-/-}$ mice are susceptible to *N. caninum* infection (51), but the impact of IL-12p40 deletion on infection kinetics was not known. To investigate the role of IL-12p40 in *N. caninum* proliferation kinetics, we first performed an exploratory experiment to test the susceptibility of IL-12p40 knockout (IL-12p40$^{-/-}$) mice to Nc1:Luc and monitored bioluminescence and survival ($n = 2$). We infected WT or IL-12p40$^{-/-}$ mice with 10^6 *N. caninum* tachyzoites, measured the parasite burden (Fig. 4A), and quantified serum IFN-γ levels. As expected, based on previous work, IL-12p40$^{-/-}$ mice were more susceptible to *N. caninum* infection than WT mice, as illustrated by increased mortality (Fig. 4B). Increased mortality correlated with significantly higher *N. caninum* parasite burdens in IL-12p40$^{-/-}$ mice than in WT mice by as early as 1 to 2 dpi (Fig. 4C and D) and remained significantly higher over the course of the infection (Fig. 4C and D). In contrast to our experiments in IFN-$\gamma^{-/-}$ mice (Fig. 3), the parasite burden declined between days 4 and 7 p.i. in IL-12p40$^{-/-}$ mice. An additional experiment ($n = 3$ per mouse strain) (Fig. 4B) confirmed our results and the

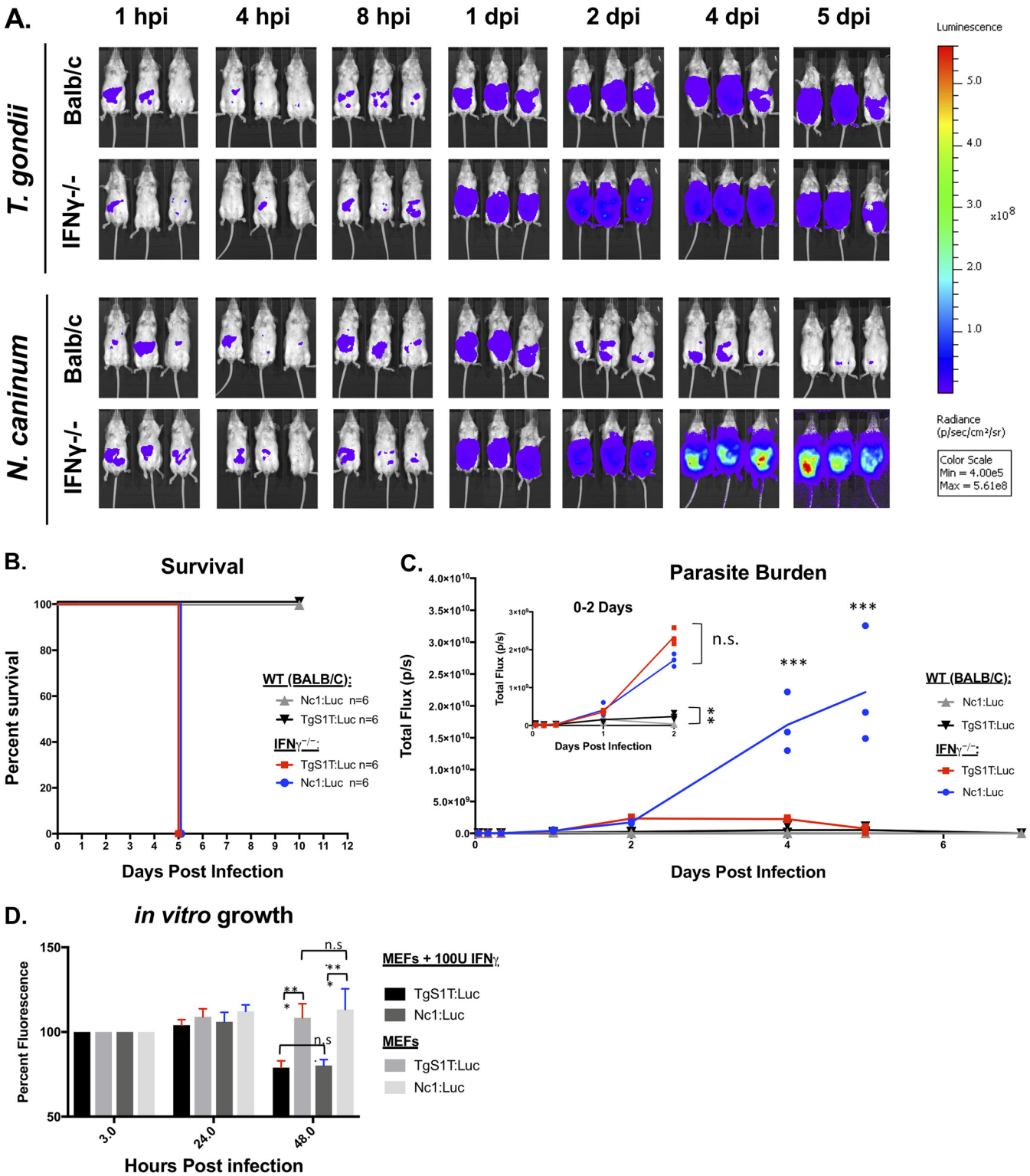

FIG 3 IFN-γ is required for control of *N. caninum* proliferation during acute infections in BALB/c IFN-$\gamma^{-/-}$ mice. Six-week-old female interferon gamma knockout (IFN-$\gamma^{-/-}$) and BALB/c control mice were infected with 10^6 TgS1T:Luc or 10^6 Nc1:Luc tachyzoites i.p. (A) Bioluminescence images showing parasite-derived luciferase signals at selected time points. (B) Combined survival of IFN-$\gamma^{-/-}$ or BALB/c mice infected with *T. gondii* or *N. caninum* (data shown are from two experimental replicates each with $n = 3$ per parasite/mouse strain). (C) BALB/c background IFN-$\gamma^{-/-}$ mice ($n = 3$ per parasite species) or WT BALB/c mice ($n = 3$ per parasite species) were infected as described above (the experiment was repeated [see Fig. S3A in the supplemental material]). (D) Mouse embryonic fibroblast cells were treated with 100 U of recombinant IFN-γ (R&D) 24 h after being inoculated with 10^4 tachyzoites of either TgS1T:Luc or Nc1:Luc. Parasite-derived DsRed fluorescence (both strains also express DsRed [see Materials and Methods]) was quantified at 3 and 24 hpi, IFN-γ was then added, and fluorescence was quantified 24 h after the addition of IFN-γ (48 h after inoculation). The first data point was normalized to 100% for display purposes. Statistical analysis was performed using two-way repeated-measures ANOVA (alpha value of 0.05) with Sidak's multiple-comparison test on the raw (nonnormalized) data. *, $P < 0.05$; **, $P < 0.01$; ***, $P < 0.001$; n.s., not significant.

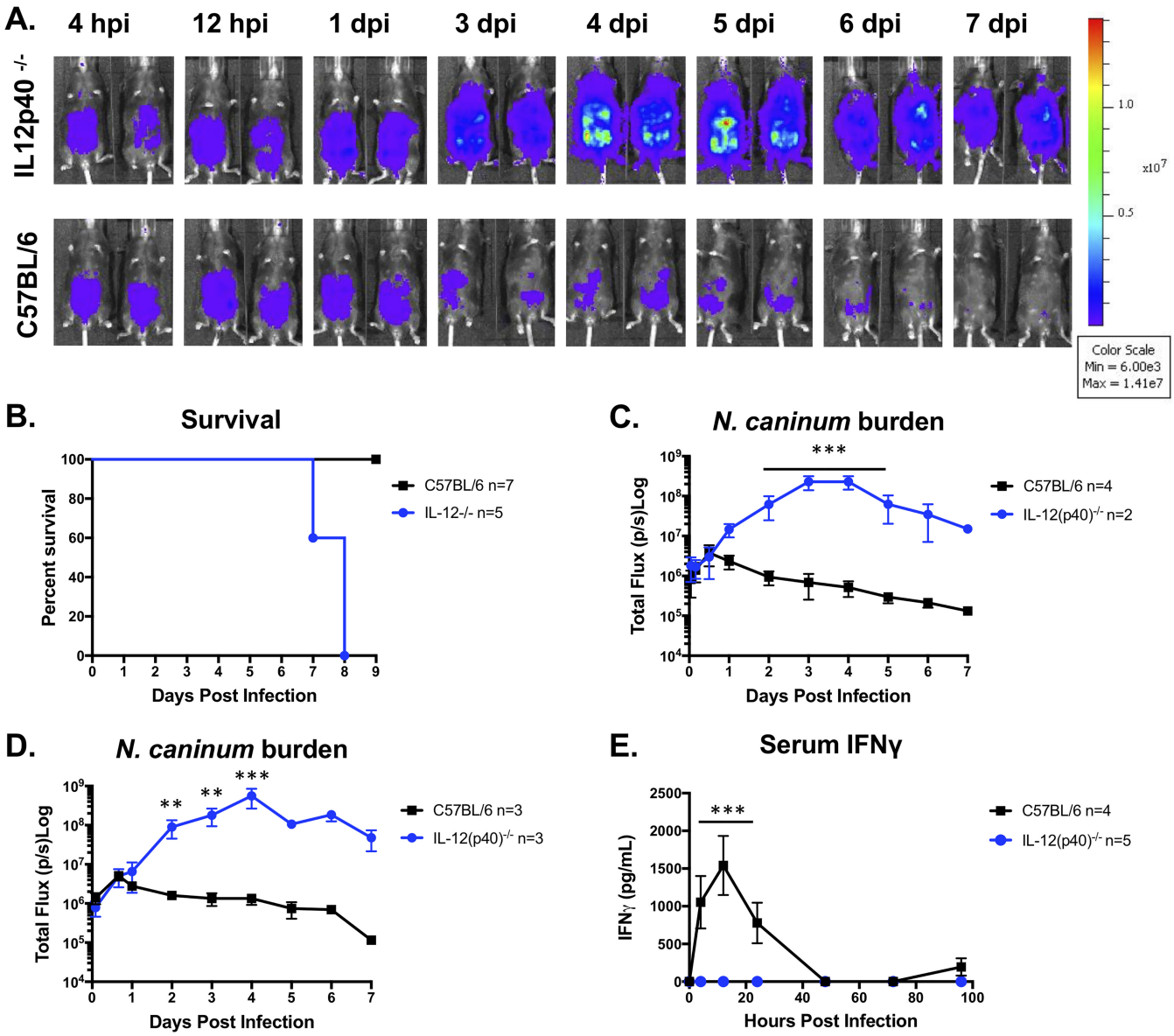

FIG 4 IL-12p40 knockout mice fail to control *N. caninum* infection but with different infection dynamics. Six-week-old C57BL/6 or IL-12p40 knockout (IL-12p40$^{-/-}$) mice were injected i.p. with 10^6 Nc1:Luc tachyzoites. (A) Bioluminescence imaging data during days 0 to 7 postinfection. Hours postinfection (hpi) and days postinfection (dpi) are indicated ($n = 2$ per mouse strain). (B) Combined survival of IL-12p40$^{-/-}$ mice compared to control mice infected with *N. caninum*. Data shown are from two experiments (IL-12p40$^{-/-}$, $n = 5$; WT, $n = 7$). (C) Quantification of bioluminescence data measuring parasite burden (total flux [photons per second]) over time ($n = 2$ per mouse strain). (D) Quantification of bioluminescence data from experimental repeats (IL-12p40$^{-/-}$, $n = 3$; WT, $n = 3$). (E) Serum samples were collected at 0, 8, 12, 24, 48, 72, and 96 hpi and analyzed with a mouse IFN-γ ELISA. No IFN-γ was detected in IL-12p40$^{-/-}$ mice. The graph combines data from two experiments (IL-12p40$^{-/-}$ mice, $n = 5$; WT mice, $n = 4$). Control mice ($n = 4$) for the experiment in panel D were infected at the same time as multiple-knockout mice, and data from serum samples taken from these same mice are also shown in Fig. 6D. Cytokines were analyzed by two-way repeated-measures ANOVA (alpha value of 0.05) with Sidak's multiple-comparison test. Imaging data were log transformed, and two-way repeated-measures ANOVA (alpha value of 0.05) and Sidak's multiple-comparison test were then performed. **, $P < 0.01$; ***, $P < 0.001$.

previously reported susceptibility of IL-12p40$^{-/-}$ mice to *N. caninum* (51). In both our experiments, IL-12p40$^{-/-}$ mice infected with *N. caninum* produced no detectable serum IFN-γ (Fig. 4E).

CCL2/MCP gene deletion does not alter the outcome of *N. caninum* infection. In our Luminex-based cytokine screen, we observed that the chemokine CCL2/MCP had an induction profile similar to those of both IFN-γ and IL-12, in that it was induced immediately (within 24 hpi) during *N. caninum* infections and not until later (e.g., 48 hpi) during infections with *T. gondii*. We reasoned that CCL2/MCP might be important for host control of *N. caninum* proliferation, as it has been previously shown that the

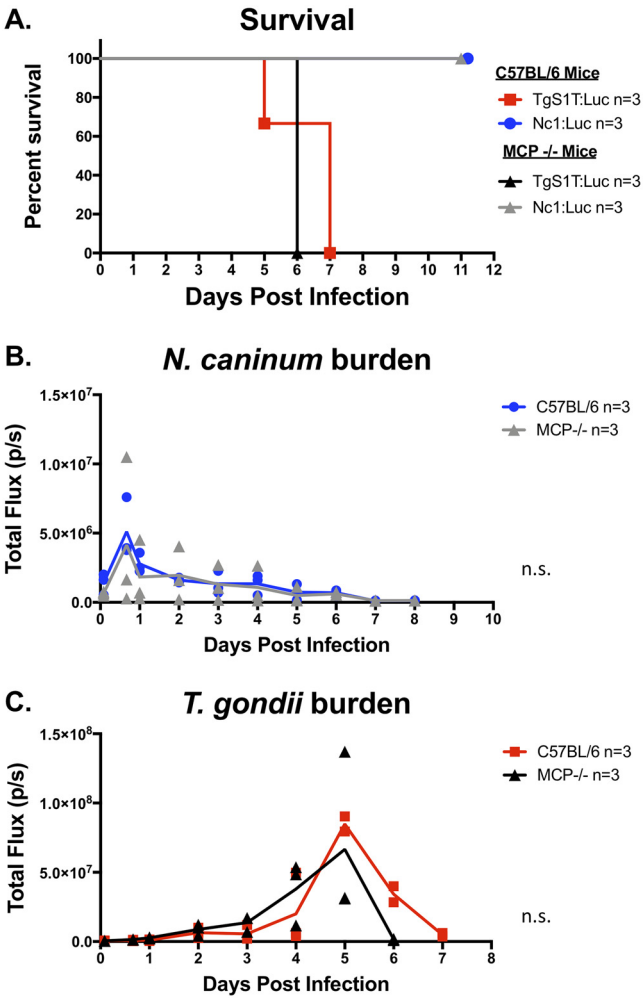

FIG 5 *In vivo* bioluminescence imaging comparing *N. caninum* and *T. gondii* acute infections in MCP (CCL2) knockout ($MCP^{-/-}$) or WT C57BL/6 mice. $MCP^{-/-}$ mice ($n = 3$ per parasite species) and C57BL/6 (control) mice ($n = 3$ per parasite species) were infected with 10^6 tachyzoites of either *N. caninum* or *T. gondii*. (A) Survival of mice throughout acute infection. (B) Parasite burden of Nc1:Luc infection in either C57BL/6 or $MCP^{-/-}$ mice. Data were log transformed, and two-way repeated-measures ANOVA (alpha value of 0.05) with Dunnett's multiple-comparison test was performed. No statistically significant differences were found in the $MCP^{-/-}$ mouse comparison for Nc1 infection. (C) TgS1T:Luc infections in C57BL/6 or $MCP^{-/-}$ mice. Data were log transformed, and two-way repeated-measures ANOVA with Dunnett's multiple-comparison test was performed. No statistically significant differences were found in the $MCP^{-/-}$ mouse comparison for TgS1T infection.

loss of CCL2/MCP enhanced susceptibility to *T. gondii* due to its role in recruiting $GR1^+$ inflammatory monocytes to the site of infection (52). To test how the genetic ablation of this chemokine would impact the proliferation of either parasite, we compared TgS1T:Luc and Nc1:Luc infections in MCP knockout ($MCP^{-/-}$) mice and measured bioluminescence signals over the course of the infection ($n = 3$ per mouse strain and parasite species). We found no difference in survival (Fig. 5A) or parasite burden (Fig. 5B) for *N. caninum* infections between WT C57BL/6 and $MCP^{-/-}$ mice. Similarly, $MCP^{-/-}$ mice infected with *T. gondii* did not exhibit significant differences in mortality compared to WT mice (Fig. 5A) and also had similar parasite burdens over the course of the experiment (Fig. 5C). These data show that MCP plays a minor, if any, role in mouse resistance to *N. caninum* (Nc1) or *T. gondii* (S1T) during the acute phase of infection at the doses used in these assays.

MyD88 is required for immediate induction of IL-12 and IFN-γ in response to *N. caninum* infection and control of *N. caninum* during the first 24 hpi. It is well

established that MyD88 is required for resistance to *T. gondii* infections in mice (53). *T. gondii* infection in MyD88$^{-/-}$ mice is characterized by uncontrolled parasite proliferation and defective IL-12 production (54). Since *N. caninum* induces a potent proinflammatory immune response within hours of infection compared to *T. gondii* infections in mice (Fig. 2), we sought to determine if host Toll-like receptor (TLR) signaling was required for early IL-12 and IFN-γ induction (Fig. 2C and F and Fig. S1B) and the control of *N. caninum* proliferation (Fig. 2A and D and Fig. S1A) *in vivo*. We first performed an exploratory experiment and infected 2 mice lacking MyD88 or WT (C57BL/6) mice with 10^6 Nc1:Luc:DsRed (Nc1:Luc) tachyzoites. Both MyD88$^{-/-}$ mice survived Nc1:Luc infection. We then performed 3 additional experiments to confirm the accuracy of our results. We observed that 100% of *N. caninum*-infected MyD88$^{-/-}$ mice survived in all four experiments (Fig. 6C [$n = 2$ per mouse strain], Fig. 6F [$n = 3$ per mouse strain], Fig. S3B [$n = 3$ per mouse strain], and data not shown [$n = 3$ per mouse strain]). We performed three of the experiments in our facility (Fig. 6A), and our collaborator performed the last experiment in another laboratory at a different institution (Fig. 6F). Our results demonstrate that MyD88 is not required for the survival of sublethal (10^6) i.p. infections with *N. caninum* (Nc1:Luc) in mice (Fig. 6A and F), a result that is in conflict with at least one previous report (51). However, when we quantified parasite burdens using *in vivo* BLI, we found that the parasite burden was mostly similar between WT and MyD88$^{-/-}$ mice during the first 24 hpi (Fig. 6B and C and Fig. S3B), with the only significant difference being higher burdens in WT than in MyD88$^{-/-}$ mice at 12 hpi (Fig. 6C). At later stages of infection, the parasite burden was significantly higher in MyD88$^{-/-}$ mice than in WT mice (Fig. 6C and Fig. S3B), suggesting that MyD88$^{-/-}$ mice have deficiencies in controlling *N. caninum* proliferation during acute infection (consistent with previous reports of MyD88$^{-/-}$ mice having increased susceptibility to *N. caninum* [51]). When we examined serum cytokine levels, we found that MyD88$^{-/-}$ mice infected with *N. caninum* did not produce detectable serum IL-12p40 or IL-12p70 over the course of the infection (Fig. 6E and Fig. S3C and D). We also did not detect IFN-γ during the first 24 h in *N. caninum*-infected MyD88$^{-/-}$ mice (in contrast to WT mice) (Fig. 6D and G and Fig. S3E), indicating the dependence of immediate serum IL-12 and IFN-γ on MyD88. Surprisingly, however, we observed significantly increased IFN-γ levels at days 3 to 5 p.i. in MyD88$^{-/-}$ mice but not in control mice (Fig. 6D and G and Fig. S3E). This increase in IFN-γ preceded a reduction of the *N. caninum*-derived bioluminescence signal between days 4 and 6 p.i. in MyD88$^{-/-}$ mice (Fig. 6C and D and Fig. S3B and E). Thus, while MyD88$^{-/-}$ mice did not produce IFN-γ during the first 3 days of *N. caninum* infection, and this coincided with a significantly higher parasite burden than in WT mice, MyD88$^{-/-}$ mice produced IFN-γ later during acute infection (4 to 5 dpi), and this correlated with what appeared to be a resolution of the infection. Importantly, we did not detect serum IL-12 (p40 or p70) at any time point during *N. caninum* infection in MyD88 knockout mice, suggesting that this "pulse" of IFN-γ was IL-12 independent.

Previous work *in vitro* has shown that *N. caninum* infection induced type I interferon responses that are dependent on TLR3 signaling (55) in human cells. Additionally, TLR3 has been shown to be important for mouse resistance to *N. caninum* (although with a different *N. caninum* strain and at a 10-fold-higher dose than those used here [56]). To investigate the possibility that type I interferons might also be produced during the immediate host response to *N. caninum*, we tested serum samples from our *in vivo* experiments for detectable IFN-α and IFN-β during the first 48 h after both *T. gondii* and *N. caninum* infections in BALB/c mice. We also tested serum and peritoneal lavage samples from MyD88$^{-/-}$ and WT C57BL/6 mice infected with *N. caninum*. We observed no significant induction of either cytokine at 4 or 8 hpi and only a slight ($\sim$100 pg/ml) induction of IFN-α in one *N. caninum*-infected BALB/c mouse at 24 hpi (Fig. S4A and B). These data suggest that type I interferons are unlikely to play a major role in driving immediate innate responses to *N. caninum*. Next, we investigated the possibility that TLR3 signaling played a role in driving early IFN-γ induction during *N. caninum* infection. We performed 2 experiments infecting TLR3 knockout (TLR3$^{-/-}$) and WT

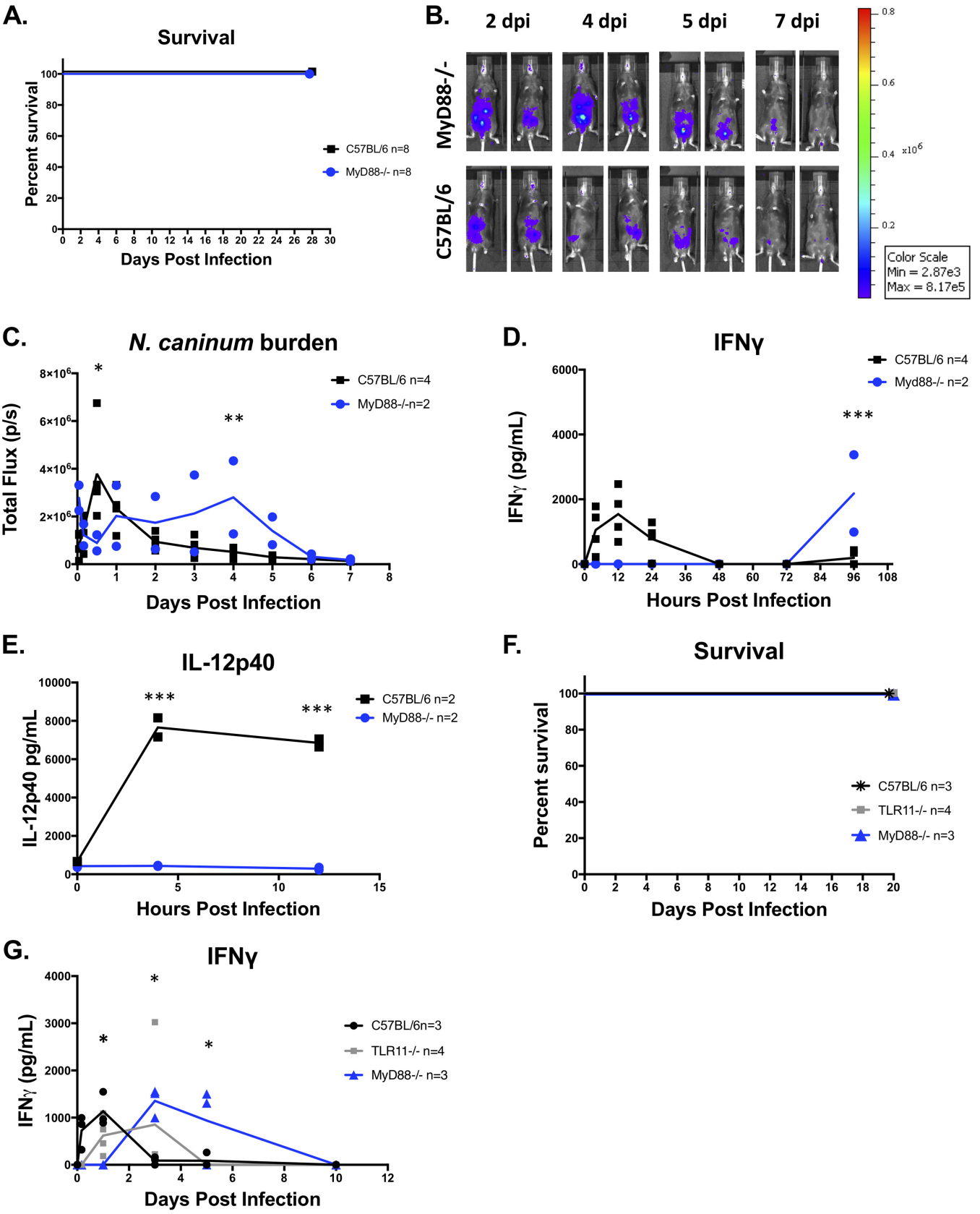

FIG 6 *In vivo* bioluminescence imaging and cytokine production in MyD88 or TLR11 knockout mice. (A) Combined survival of MyD88$^{-/-}$ or C57BL/6 mice infected with 10^6 Nc1:Luc tachyzoites from 3 experiments ($n = 8$ per mouse strain). (B) Bioluminescence imaging of Nc1:Luc infections. The control mice shown are also shown in Fig. 4A, as multiple-knockout mice were tested at the same time. (C) Quantification of bioluminescence imaging ($n = 2$ per mouse strain) (the

(Continued on next page)

(C57BL/6) mice with 10^6 *N. caninum* tachyzoites and monitored parasite burdens (Fig. S4C [TLR3$^{-/-}$, $n = 2$; WT, $n = 3$] and Fig. S4E [TLR3$^{-/-}$, $n = 3$; WT, $n = 2$]). Overall, we found that TLR3$^{-/-}$ mice were not more susceptible to *N. caninum* than WT mice. In fact, we found that the *N. caninum* parasite burden was significantly lower in TLR3$^{-/-}$ mice than in control mice at either 8 hpi ($P < 0.0001$) (Fig. S4C) or 4 hpi ($P < 0.05$) (Fig. S4E). We also found that, unlike MyD88$^{-/-}$ mice, TLR3$^{-/-}$ mice were capable of producing immediate (4 hpi) IFN-γ in response to *N. caninum* infection (Fig. S4D and F). TLR3$^{-/-}$ mice produced significantly ($P < 0.05$) less IFN-γ at 4 hpi than did control mice in one (Fig. S4D) out of two (Fig. S4F) experiments. Overall, we found that TLR3 signaling is not required for most, if not all, of the immediate induction of IFN-γ in response to *N. caninum*. These results indicate that while previous reports suggest that TLR3 and IFN-α/IFN-β may have a role in the response of human cells to *N. caninum*, we did not find any evidence that these pathways are required for immediate IFN-γ induction or for host resistance to *N. caninum* in the mouse model of infection.

Mice deficient in TLR11 do not produce immediate IFN-γ during *N. caninum* infections. *T. gondii* profilin, an essential actin-binding protein required for parasite invasion, is recognized by TLR11 (57) in mice, generating a potent TLR11-dependent IL-12 response (58). *N. caninum* has a gene that is a clear ortholog of the *T. gondii* profilin gene; *N. caninum* profilin (*NCLIV_000610*) shares over 95% amino acid identity with *T. gondii* profilin (Fig. 7A), and both also have tachyzoite transcript abundance levels in the top 5% of all genes queried by transcriptome sequencing (RNAseq) (15) (ToxoDB [https://toxodb.org/toxo/]). However, to date, it is not known if TLR11 is important for innate immune recognition during *N. caninum* infection. To address the possibility that *N. caninum* profilin is responsible for immediate host recognition resulting in the robust production of IFN-γ and IL-12 within hours of infection, we infected 4 TLR11$^{-/-}$, 3 MyD88$^{-/-}$, or 3 WT mice with 10^6 Nc1:Luc tachyzoites and tested serum samples for cytokine induction over the course of the infection. As with *T. gondii* infection (57), all TLR11$^{-/-}$ mice survived *N. caninum* infection (Fig. 6F), and we found that by 4 hpi, both TLR11$^{-/-}$ and MyD88$^{-/-}$ mice had significantly lower serum IFN-γ levels than did WT mice (Fig. 6G). However, by 24 hpi, serum IFN-γ levels in TLR11$^{-/-}$ mice rose to levels that were similar to those observed in WT mice (Fig. 6G). This suggested that unlike TLR3, TLR11 may play at least a partial role in the immediate induction of IFN-γ during *N. caninum* infection, but there may be additional MyD88-dependent host factors required (such as TLR12).

Expression of *N. caninum* profilin in *T. gondii* ME49 does not result in early induction of IFN-γ. Serum IFN-γ was not detected in mice lacking TLR11 or MyD88 during the first few hours of infection, consistent with deficiencies in innate TLR sensor recognition mechanisms. *T. gondii* profilin is known to interact with mouse TLR11, resulting in an IL-12-driven immune response (58). Alignments indicate that profilin is highly conserved between *T. gondii* and its close relatives (59), although it has 4 amino acid polymorphisms in a region of the protein previously shown (59) to be required for TLR11 activation (Fig. 7A, green box). We hypothesized that the immediate induction of IFN-γ in *N. caninum*-infected mice was due to the observed differences in the profilin sequences. To test this hypothesis, we expressed a C-terminally hemagglutinin (HA)-tagged version of either *N. caninum* or *T. gondii* profilin in *T. gondii* (ME49 strain) from a highly active GRA1 promoter (60) and quantified its impact on the host innate response or parasite proliferation in mice. Using immunofluorescence microscopy, we found that both *T. gondii* and *N. caninum* HA-tagged profilins were expressed at similar

FIG 6 Legend (Continued)
experiment was repeated [see Fig. S3B in the supplemental material]). Bioluminescence data were log transformed, and two-way repeated-measures ANOVA (alpha value of 0.05) with Dunnett's multiple-comparison test was performed. (D and E) Serum samples were collected at 0, 8, 12, 24, 48, 72, and 96 hpi and analyzed for IFN-γ (D) or IL-12p40 (E) by an ELISA ($n = 2$ per mouse strain and time point) (the experiment was repeated [Fig. S3]). (F) Survival data for MyD88$^{-/-}$ ($n = 3$), TLR11$^{-/-}$ ($n = 4$), and WT (C57BL/6) ($n = 3$) mice infected with Nc1:Luc. (G) IFN-γ concentrations in serum samples from Nc1:Luc-infected TLR11$^{-/-}$, MyD88$^{-/-}$, or WT (C57BL/6) mice. Cytokine data were analyzed using two-way repeated-measures ANOVA (alpha value of 0.05) with Sidak's multiple-comparison test. *, $P < 0.05$; **, $P < 0.01$; ***, $P < 0.001$.

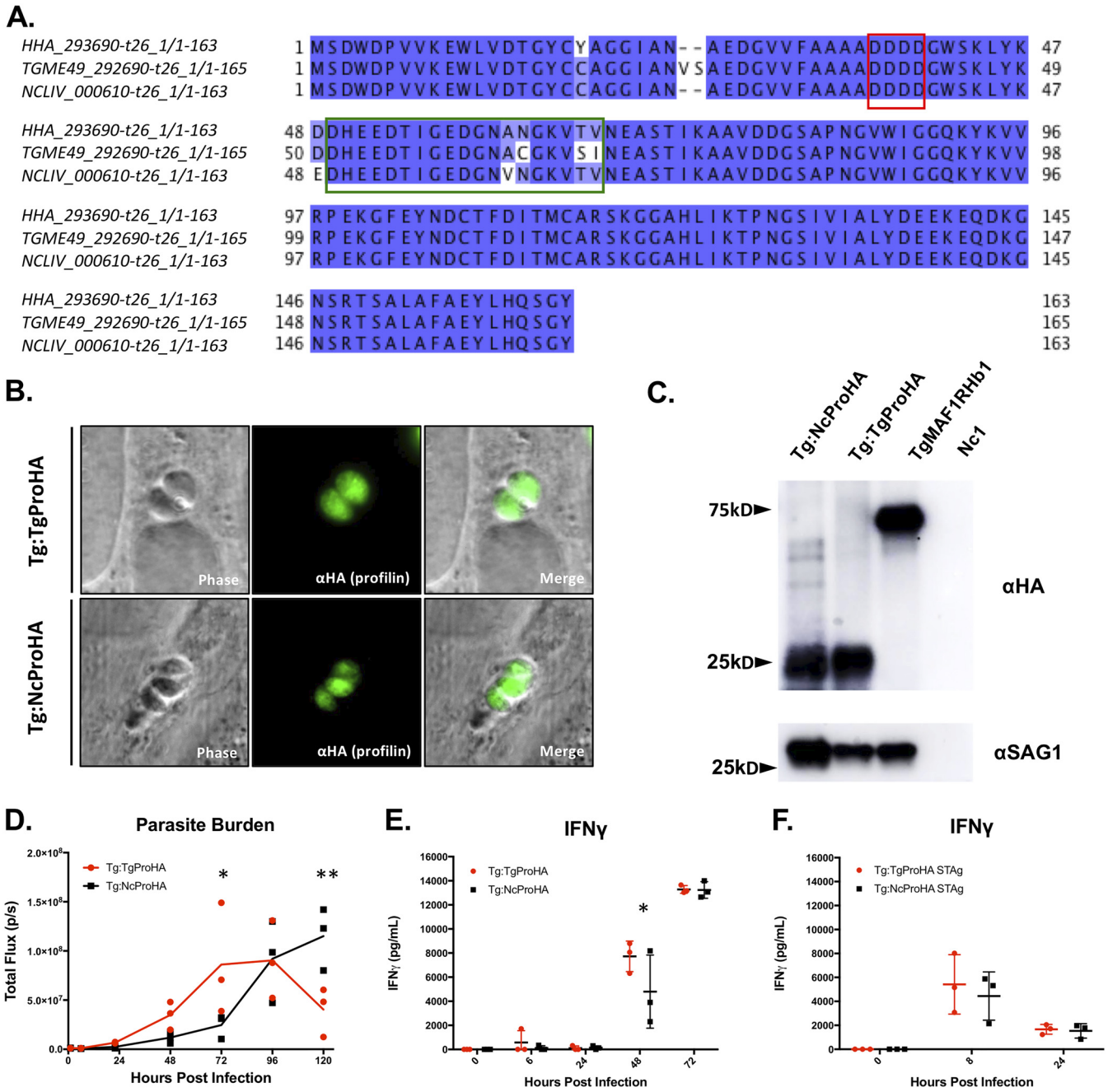

FIG 7 IFN-γ production and *in vivo* bioluminescence imaging of transgenic *T. gondii* ME49 expressing either *T. gondii* or *N. caninum* profilin. (A) Alignment of the *T. gondii* profilin predicted amino acid sequence with those from the near relatives *N. caninum* and *Hammondia hammondi*. Putative substrate-binding motifs identified previously by Kucera and colleagues (59) are outlined as follows: the red box indicates an acidic loop (AL), and the green box indicates a β-hairpin. Sequences were obtained from ToxoDB (*H. hammondi* HHA_293690, *T. gondii* TGME49_293690, and *N. caninum* NCLIV_000610). (B) Anti-HA immunofluorescence assay (IFA) of ME49:TgProfilinHA (Tg:TgProHA) (top row) or ME49:NcProfilinHA (Tg:NcProHA) (bottom row) showing the expected cytoplasmic localization. (C) Western blotting using anti-HA (top blot) or anti-SAG1 (bottom blot) as a loading control. Arrows indicate sizes in kilodaltons. (D to F) Six- to eight-week-old BALB/c mice were infected with 10^6 tachyzoites ($n = 3$ per parasite strain) or injected with soluble tachyzoite antigen (STAg) preparations equivalent to 10^6 tachyzoites of the indicated parasite strains ($n = 3$ per parasite strain). (D) Quantification of bioluminescence imaging (total flux [photons per second]) over the time course of infection of mice with Tg:TgProHA or Tg:NcProHA. Data were log transformed, and two-way repeated-measures ANOVA (alpha value of 0.05) with Sidak's multiple-comparison test was performed (analyses were performed on days 0 to 5). (E) IFN-γ ELISA of samples collected over the course of infection with Tg:TgProHA or Tg:NcProHA. Two-way repeated-measures ANOVA (alpha value of 0.05) and Sidak's multiple-comparison test were performed. (F) IFN-γ ELISA of samples collected after injection of Tg:TgProHA STAg or Tg:NcProHA STAg. Two-way repeated-measures ANOVA (alpha value of 0.05) with Sidak's multiple-comparison test was performed (analysis for 0 to 48 h). No statistically significant differences were identified between mice injected with Tg:TgProHA STAg and those injected with Tg:NcProHA STAg. *, $P < 0.05$; **, $P < 0.01$.

levels in *T. gondii* and localized to the parasite cytoplasm (Fig. 7B). We also found that both proteins were detectable at the expected apparent molecular weight (20 to 30 kDa) by Western blotting (Fig. 7C). Normalization to *T. gondii* SAG1 indicated that the *T. gondii* profilin gene was expressed at ~2-fold-higher levels than the *N. caninum* gene (Fig. 7C). When we infected 3 mice per parasite strain with 10^6 *T. gondii* tachyzoites expressing either *T. gondii* TgME49:TgProHA (Tg:TgProHA) or *N. caninum* TgME49:NcProHA (Tg:NcProHA) profilin, we observed no significant differences in parasite burdens during the first 48 hpi, but we observed a slight but significant reduction in the Tg:NcProHA burden compared to the Tg:TgProHA burden (Fig. 7D). Regarding IFN-γ production, we observed no significant differences in serum IFN-γ levels at most queried time points (Fig. 7E). The only exception was a significantly higher abundance of IFN-γ in Tg:TgProHA-infected mice than in Tg:NcProHA-infected mice at 48 hpi (Fig. 7E). Consistent with the cytokine data, we also found no differences in host survival (all infected mice succumbed to the infection by day 8 p.i., as expected for this dose and strain), but our observation of a significantly reduced parasite burden for Tg:NcProHA compared to Tg:TgProHA at both and 3 and 5 dpi (Fig. 7D) suggests that there may be moderate differences in *N. caninum* and *T. gondii* profilins that might impact infection outcomes. However, these differences do not correlate with any differences in the production of IFN-γ and therefore are unlikely to be the main driver of the dramatic phenotypic differences in the host response and resistance to these two parasite species. Since we saw no difference in IFN-γ production during the first 24 h of infection, we sought to confirm this negative result and eliminate the possibility that profilin release was somehow altered in our transgenic parasites. Since profilin activity can be assayed directly by the injection of soluble tachyzoite antigen (STAg) (61, 62), we injected 3 mice per parasite strain with STAg equivalent to 10^6 parasites of either Tg:TgProHA or Tg:NcProHA and quantified IFN-γ production. We observed no statistically significant differences in serum IFN-γ concentrations between mice injected with parasites expressing HA-tagged *T. gondii* profilin and those expressing HA-tagged *N. caninum* profilin (Fig. 7F), suggesting that differences in the profilin coding sequences between these species are not sufficient to account for their dramatic differences in IFN-γ induction and host control during the first 24 hpi in mice.

DISCUSSION

The *T. gondii-N. caninum* comparative system provides a unique opportunity to address the question of host compatibility at the molecular level using the genetically tractable mouse model to compare two parasites with a close phylogenetic relationship, conserved gene content, and yet dramatic differences in disease outcomes. Our results add to a growing body of work indicating that both *T. gondii* and *N. caninum* rely on IFN-γ for resistance to infection and are consistent with the key role that this cytokine plays in immunity to intracellular pathogens (63, 64). What we found to be surprising was the fact that *N. caninum* induced a potent IFN-γ response in the hours immediately following infection, while *T. gondii* did not, a fact that has not been appreciated prior to our comparative analyses. This is somewhat paradoxical since *T. gondii* infection is characterized by remarkably high IFN-γ levels in the later stages of infection, which exceed those observed in *N. caninum* infections by ~10-fold. At this stage of infection, *T. gondii* growth is protected to various degrees by an extensive array of *T. gondii*-secreted effectors that disrupt IFN-γ-mediated parasite killing, such as rhoptry kinases 5, 18, and 17 (39, 65, 66) and dense granule proteins like IST (inhibitor of STAT transcription) (67, 68). The lack of IFN-γ induction during the first 48 h after *T. gondii* infection has not previously been examined in a comparative context as we have done here, leading to an important question as to how *T. gondii*, but not *N. caninum*, avoids and/or suppresses this robust and rapid IFN-γ response.

In IFN-$\gamma^{-/-}$ mice, *N. caninum*-derived luciferase activity rose to levels that were 10-fold higher than those observed in *T. gondii*-infected IFN-$\gamma^{-/-}$ mice (Fig. 3C). It is unlikely that this difference in luciferase signals was due to differences in luciferase production by *N. caninum* compared to *T. gondii*, rather than a difference in the actual

parasite burden, since we observed similar baseline luciferase levels between these parasite species during the first 24 hpi in WT mice and by as late as 2 dpi in IFN-$\gamma^{-/-}$ mice (Fig. 3C). The difference in burdens observed in IFN-$\gamma^{-/-}$ mice might seem surprising given the lack of host-pathogen compatibility between *N. caninum* and the mouse, but it makes sense in the context of (i) a reliance on IFN-γ for protection and (ii) there having been little, if any, opportunity for host-pathogen coevolution between *N. caninum* and the murine host. Compared to its extensive interactions with *T. gondii*, the mouse has not developed countermeasures against *N. caninum* outside IFN-γ production, since, as we clearly show, this is a highly effective mechanism of *N. caninum* control and overall fails to control *T. gondii*. Once this immunological barrier is removed, the markedly enhanced replication of *N. caninum* may be due to the absence of any additional parasite-specific defenses. From our comparative studies, an important question emerges as to what additional countermeasures are restricting *T. gondii* growth in the absence of IFN-γ. The mouse may recognize other *T. gondii*-derived antigens via innate immune receptors, leading to the recruitment of other parasiticidal host cells and/or the production of other proinflammatory cytokines with effector function. One such effector could be nitric oxide, which is important for resistance against chronic *T. gondii* infection in mice (69) but can be actively suppressed by *T. gondii* in a variety of contexts, suggesting the existence of an ongoing molecular arms race (70, 71). The *N. caninum*-*T. gondii* comparative model may be an effective system to identify what these differences may be and allow the discovery of unique, IFN-γ-independent mechanisms of intracellular eukaryotic pathogen elimination.

Previous work showed that MyD88 was required for mouse survival of infection with 10^6 "viable" tachyzoites of *N. caninum* (Nc1 strain) (51), where the number of viable tachyzoites was determined using trypan blue exclusion. In the present study, we found that all MyD88$^{-/-}$ mice survived infection with 10^6 *N. caninum* tachyzoites (Fig. 6). This discrepancy is most likely due to differences between the studies in how the dose was determined. For our studies, we did not normalize input parasites by dye exclusion, but based on plaque assays for these studies, we typically observe ~10 to 20% viability of input parasites. Therefore, it is likely that our "effective" dose is significantly lower than 10^6 tachyzoites, and this is why we did not observe any mortality while others did (including a more recent study showing 100% mortality in MyD88$^{-/-}$ mice infected with 10^7 total *N. caninum* tachyzoites [56]).

Despite this discrepancy, other aspects of those studies (51, 56) are consistent with our results. For one, our data clearly show increased susceptibility to *N. caninum* in MyD88 knockout mice based on higher parasite burdens at the later stages of acute infection (Fig. 6C; see also Fig. S3B in the supplemental material). *N. caninum* infection led to increased IL-12p40 and IFN-γ levels in peritoneal exudates by day 3 p.i., and this induction was dependent on MyD88 (51). The level of IL-12p40 was also higher in serum samples taken from *N. caninum*-infected WT mice by day 3 p.i. than at day 0, and this increase persisted over the course of the experiment and was also dependent on MyD88. In contrast to our work, serum IFN-γ was not detected in that study until day 7 p.i. and was only moderately dependent on MyD88 (51). Our study supplements that previous work by showing that immediate IL-12 (both p40 and p70) and IFN-γ are highly dependent on MyD88 and that late IFN-γ is observed in response to *N. caninum* only in MyD88$^{-/-}$ mice and therefore is not dependent on MyD88. Although IL-12p40 is also a subunit of IL-23 (72), our results demonstrate that the biologically active form, IL-12p70, is absent during immediate infection in the absence of MyD88. These results suggest two phases of the IFN-γ response to *N. caninum*: (i) an immediate response can be sufficient to effectively control the parasite under the dosing regimen used (10^6 total tachyzoites), and (ii) if the infection is not effectively controlled by this immediate response (as in MyD88$^{-/-}$ mice), a later wave of IFN-γ can promote parasite control and mouse survival (Fig. 6D). In the present study, the comparatively higher lethality in MyD88$^{-/-}$ mice observed previously (51) suggests that the lack of immediate control in MyD88$^{-/-}$ mice led to an increased proliferation of the parasite at levels that overwhelmed the mouse by days 12 to 15 p.i. due to the higher effective inoculum (10^6

trypan blue-negative parasites versus 10^6 total tachyzoites in the present study). Differences in inocula and parasite strains may also contribute to the differences between the present study and another showing that TLR3 knockout mice were more susceptible to *N. caninum* than were WT mice (in this case after infection with 10^7 tachyzoites [56]). In our study, we observed small differences in parasite burdens and IFN-γ levels at 4 hpi and no impact on parasite control in TLR3$^{-/-}$ mice, as *N. caninum* infections were controlled within the same time frame as in WT mice. We also failed to detect any evidence that type I interferons were being significantly induced by *N. caninum* in mice (in contrast to human cells [55]).

It is interesting that in our study, the same pattern did not occur in IL-12p40$^{-/-}$ mice. While these mice failed to mount an immediate response to *N. caninum*, we never observed detectable levels of serum IFN-γ. Overall, if differences in parasite preparation are taken into account, our study and the previous report (51) are complementary, in that ours focuses on differences in the immediate (i.e., within 24 h) responses to infection, while the previous study focuses more on later responses (i.e., from day 3 p.i. onward).

Since the immediate IFN-γ response elicited by *N. caninum* was dependent upon MyD88 and IL-12, we reasoned that TLR11 recognition of *N. caninum* may be an important sensor required for IFN-γ production in the first 24 h, thus contributing to *N. caninum* incompatibility in mice. Although early (4 hpi) IFN-γ production was not detected in TLR11$^{-/-}$ mice, TLR11$^{-/-}$ mice produced serum IFN-γ beginning at 24 hpi, suggesting that TLR11 is not the only MyD88-dependent recognition mechanism capable of contributing to the production of critical IFN-γ required to control *N. caninum*. The most likely candidate for mediating this immediate response to *N. caninum* is TLR12, another MyD88-dependent TLR known to be capable of recognizing *T. gondii*-derived pathogen-associated molecular patterns (PAMPs), including the TLR ligand profilin (59, 61, 73).

Given the dependence of immediate IFN-γ during *N. caninum* infection on MyD88 and TLR11, profilin was a likely candidate gene to mediate the observed differences in the host response and resistance to *N. caninum* infection. We were encouraged to test this hypothesis based on the existence of multiple amino acid differences between the predicted *T. gondii* and *N. caninum* profilin gene products in a β-hairpin region of the protein shown previously to be required for interactions with TLR11 (59). Since our aim was to identify any differences in the biology of *N. caninum* profilin compared with that of *T. gondii* in the immediate production of IFN-γ, we reasoned that the transgenic expression of *N. caninum* profilin would reveal dominant antigenic properties associated with innate IFN-γ production. By using a parasite expression system, we remove issues that arise from bacterial expression constructs, including bacterial activation of host immune responses and posttranslational modification differences. Using both live parasites as well as STAg preparations, we did not observe differences in cytokine production or parasite burden, consistent with the immediate induction of IFN-γ by *N. caninum* (and not *T. gondii*) being driven solely (or even in part) by differences in the profilin gene. This observation is consistent with previous work testing various apicomplexan profilins as antigen or adjuvant components for bovine vaccines (74). In those studies, recombinant *N. caninum* profilin (rNcPro) was unable to induce sufficient cell-mediated responses to provide protection in mice (75), and although it has been shown that rNcPro produced in *Escherichia coli* results in IFN-γ production, nonrecombinant protein controls (6 and 24 hpi) also induced IFN-γ production in those experiments (76). Therefore, it seems likely that there are other ligands in *N. caninum* that contribute to immediate cytokine induction and control of *N. caninum*, and their identification may require further characterization through biochemical purification and mass spectrometry. These may be additional TLR ligands or other microbe-associated molecular pattern-bearing molecules that require, at a minimum, the adaptor protein MyD88.

We do not yet know what cell type in the mouse is producing immediate (4 hpi) IFN-γ in response to *N. caninum*. Recent work investigated IFN-γ-producing cells in

adipose tissue at later time points (24 hpi, 7 dpi, 21 dpi, and 12 months) after infection but did not identify sources of IFN-γ immediately after infection responsible for controlling the *N. caninum* parasite burden (77). During the acute phase of *T. gondii* infection, much of the IFN-γ is produced by natural killer cells (23, 37), although neutrophils have recently been implicated in providing TLR11-independent IFN-γ during *T. gondii* infection (78). Regardless of the nature of the *N. caninum*-derived signal, it is a critical determinant of the incompatibility between *N. caninum* and the mouse. While it could be recognized via mechanisms similar to the ones used for *T. gondii* recognition, our results suggest that the mechanisms may be distinct or at least not fully overlapping. This idea finds support given the extensive coevolution that has occurred between *T. gondii* and the murine host and the dramatic and highly protective response to *N. caninum* that *T. gondii* manages to circumvent. Once molecules required for parasite recognition and immunity are identified and compared between *T. gondii* and *N. caninum*, it will be possible to dissect the molecular evolutionary events that led to the divergent host ranges of these two important animal parasites.

MATERIALS AND METHODS

Parasite maintenance and preparation. Parasite strains (*Toxoplasma gondii* TgS1T:Luc:DsRed, TgS23:Luc:DsRed, and TgME49 and *Neospora caninum* Nc1:Luc:DsRed) were maintained by serial passage in human foreskin fibroblasts (HFFs) isolated from pooled donated foreskins from newborns in ~2003 at Stanford Hospital. These tissues are 100% deidentified and do not entail any human subject research. HFFs were grown in Dulbecco's modified Eagle medium (DMEM) supplemented with 10% fetal bovine serum, penicillin (100 U/ml), streptomycin (100 μg/ml), and L-glutamine (2 mM) (complete DMEM [cDMEM]). Cells were grown in humidified 5% CO_2 incubators at 37°C. Monolayers were washed with phosphate-buffered saline (PBS) (for *in vivo* infections) or cDMEM (for cell culture infections), lysed by serial passage through 25- and 27-gauge needles, pelleted by centrifugation at 800 × *g* for 10 min, resuspended in 3 ml PBS or cDMEM, and then quantified by counting on a hemocytometer. Parasites were then either concentrated by centrifugation or serially diluted in PBS or cDMEM. Parasites were used at various concentrations for *in vivo* or *in vitro* assays, as described below. Plaque assays were routinely used to verify the similarity of the inocula.

Soluble tachyzoite antigen preparation. Soluble tachyzoite preparations of 1×10^7 parasites/ml were prepared based on previously reported protocols and specifically as follows. Monolayers of well-infected confluent HFF cells were washed, scraped, and lysed using 25-gauge and 27-gauge needles and then filtered through a 5-μm filter. Parasites were counted, resuspended in PBS at the desired concentration, and then frozen at −80°C. After thawing on ice, preparations were sonicated using a model FB10 sonic dismembrator (Fisher Scientific) for 20-s bursts on ice (4 times) with 1-min rests (amplitude of 20). After sonication, the samples were centrifuged for 5 min at 10,000 × *g*. The supernatant was removed, and 200 μl was injected intraperitoneally (i.p.) into each mouse.

Transgenic *T. gondii* and *N. caninum* strains. *T. gondii* strains and TgS23:GFP:Luc were described previously (26). For *T. gondii* strain TgS1T, we identified it as a potentially avirulent strain based on its genotype at key virulence loci. Specifically, based on existing F1 progeny genotype and virulence phenotype data from two distinct type II × type III crosses (39, 48), we identified TgS1T as one of the strains lacking "virulent alleles" for 5 previously characterized virulence quantitative-trait loci (39). *T. gondii* S1T and *N. caninum* NC1 were generated by transfection with a plasmid encoding DsRed and click beetle luciferase (Luc) and carrying a bleomycin resistance gene, selected using 2 to 3 rounds of bleomycin exposure (as previously described [1, 79]), and cloned by limiting dilution. All luciferase-positive clones were screened for similar levels of luciferase activity prior to use in *in vivo* bioluminescence experiments.

To generate exogenous profilin expression constructs and transgenic parasites, *N. caninum* (Liverpool strain) or *T. gondii* (ME49) profilin genes were PCR amplified from genomic DNA using primers gaaatc aagcaagatgcaATGTCCGACTGGGACCCTG and acgtcgtacgggtacCCAGACTGGTGAAGATACTCGG for *T. gondii* profilin and primers gaaatcaagcaagatgcaATGTCGGACTGGGATCCC and acgtcgtacgggtacCCAGACTGG TGAAGGTAC for *N. caninum* profilin (lowercase letters indicate primers designed for Gibson assembly cloning). DNA fragments were cloned downstream of the GRA1 promoter and in frame with a C-terminal HA tag into pGRA-HA-HPT using Gibson assembly after plasmid digestion with NsiI and NcoI (39). To generate transgenic parasites, 2×10^7 ME49:ΔHPT:Luc parasites were passed through 25- and 27-gauge needles and pelleted at 800 × *g* for 10 min. Parasites were resuspended in a solution containing glutathione (GSH), ATP, and Cytomix (0.15 mM $CaCl_2$, 120 mM KCl, 25 mM HEPES, 2 mM EDTA, 5 mM $MgCl_2$, 10 mM KPO_4 [pH 7.6]) and electroporated with 30 to 50 μg of the relevant plasmid at 25 μF and 1.6 kV. Transfected parasites were selected using cDMEM supplemented with mycophenolic acid-xanthine (MPA-Xan). Clones were obtained by limiting dilution and confirmed by immunofluorescence assays (IFAs) and Western blotting, using SAG1 as a loading control.

Animal experiments. Experiments were performed with 4- to 8-week-old female mice of strains C57BL/6J, BALB/cJ, C.129S7(B6)-*Ifng*^{tm1Ts}/J, B6.129S7-*Ifng*^{tm1Ts}/J, B6.129S1-*Il12b*^{tm1Jm}/J, B6.129S4-Ccl2tm1Rol/J, and B6.129P2(SJL)-*Myd88*$^{tm1.1Defr}$/J obtained from Jackson Laboratories, with the exception

of the TLR11$^{-/-}$ mice, which were described previously (57) and are maintained by the Yarovinsky laboratory.

***In vivo* bioluminescence assays.** We infected 4- to 8-week-old female mice (BALB/c, C57BL/6, and various knockout lines, as indicated; Jackson Laboratories) via i.p. injection of 10^6 Luc-expressing parasites in 200 μl sterile PBS. Acute infections were monitored using bioluminescence imaging by injecting mice with 3 mg D-luciferin in 200 μl sterile PBS. Images were taken using the Ivis Lumina II imaging system (Xenogen Corporation) for 4 min using maximum binning. Images were analyzed using Living Image software to calculate total flux (photons per second) across the entire body of the mouse.

***In vitro* bioluminescence assays.** For *in vitro* growth assays, confluent HFFs or MEFs in 96-well plates were infected with 10^4 *T. gondii* or *N. caninum* parasites per well and quantified using a fluorescence imaging reader (BioTek Cytation5). For HFF growth comparisons, cells were infected, and fluorescence was measured after infection and at 24 to 48 hpi. For fluorescence assays, murine embryonic fibroblasts were treated with 100 U/ml of recombinant mouse IFN-γ (R&D) 24 h after inoculation with 10^4 parasites. Cells were inoculated with 10^4 TgS1T:Luc:DsRed or Nc1:Luc:DsRed parasites per well, and fluorescence was read at the specified time points throughout the experiment (3, 24, and 48 hpi).

Cytokine and chemokine detection and analysis. Mouse chemokine and cytokine levels were measured using enzyme-linked immunosorbent assays (ELISAs) or by Luminex assays at the University of Pittsburgh Medical Center CFP Luminex Core Laboratory. The cytokine response profile is a commercially available panel that measures 32 mouse chemokines and cytokines. Commercially available ELISA kits were obtained from BD Biosciences (IL-12p40 and IFN-γ) and used according to the manufacturer's instructions.

Immunofluorescence. Coverslips (12 mm) were seeded with HFFs in 24-well plates and grown in cDMEM as described above. Coverslips were infected with *T. gondii* ME49 parasites exogenously expressing *T. gondii or N. caninum* profilin (Tg:TgProHA and Tg:NcProHA). Infected HFFs on coverslips were incubated overnight, washed with PBS, and fixed with 4% paraformaldehyde in PBS for 20 min. Following fixation, cells were blocked and permeabilized in PBS containing 5% bovine serum albumin (BSA) and 0.1% Triton X-100 for 1 h. Fixed cells were then stained with commercially obtained antibodies for HA.

Western blotting. Parasites were grown in HFF cultures as described above. Cultures were lysed using a 5-μm syringe to release parasites, filtered to remove host cell debris, washed in PBS, and then suspended in lysis buffer. Proteins were resolved by SDS-PAGE, transferred onto a nitrocellulose membrane, and blocked for 1 h in 5% BSA in PBS-Tween 20 (PBS-T). Primary antibody incubation was performed in blocking buffer for 60 min, followed by three washes in PBS-T. Anti-HA antibody (anti-HA high-affinity rat monoclonal clone 3F10, catalog number 11867431001; Sigma-Aldrich) and *T. gondii* SAG1 antibody (monoclonal mouse D61S, catalog number MA5-18268; Thermo Fisher) were used at 1:1,000 dilutions. Secondary antibody incubation was performed with horseradish peroxidase-conjugated secondary antibodies to the respective primary antibodies in blocking buffer for 45 min. Bands were visualized with the West Pico chemiluminescent substrate (Thermo Fisher).

Statistical analysis. All statistical analyses were performed using Prism 7 (GraphPad Software, Inc.). Statistical tests were chosen based on experimental design. Analyses included two-way repeated-measures analysis of variance (ANOVA) (alpha value of 0.05) with Sidak's multiple-comparison test, two-way repeated-measures ANOVA (alpha value of 0.05) with uncorrected Fisher's least significant difference (LSD) test, or two-way repeated-measures ANOVA (alpha value of 0.05) with Dunnett's multiple-comparison test. Statistical methods are described in the figure legends where appropriate. All bioluminescence data were log transformed prior to analysis.

Ethics statement. All animal procedures in this study met the standards of the American Veterinary Medical Association and were approved locally under University of Pittsburgh Institutional Animal Care and Use Committee protocol number 12010130. The animal protocol meets the National Institutes of Health (NIH) *Public Health Service Policy on Humane Care and Use of Laboratory Animals* (80) and U.S. Department of Agriculture (USDA) animal welfare regulation (AWR) guidelines.

SUPPLEMENTAL MATERIAL

Supplemental material is available online only.

SUPPLEMENTAL FILE 1, PDF file, 0.8 MB.

ACKNOWLEDGMENTS

This work was supported by NIH grant RO1AI114655 (J.P.B.) and NIH grants AI121090 and AI136538 (F.Y.). This project used the UPMC Hillman Luminex Core facility, which is supported in part by award P30CA047904.

REFERENCES

1. English ED, Adomako-Ankomah Y, Boyle JP. 2015. Secreted effectors in Toxoplasma gondii and related species: determinants of host range and pathogenesis? Parasite Immunol 37:127–140. https://doi.org/10.1111/pim.12166.
2. Collantes-Fernandez E, Arrighi RBG, Álvarez-García G, Weidner JM, Regidor-Cerrillo J, Boothroyd JC, Ortega-Mora LM, Barragan A. 2012. Infected dendritic cells facilitate systemic dissemination and transplacental passage of the obligate intracellular parasite Neospora caninum in mice. PLoS One 7:e32123. https://doi.org/10.1371/journal.pone.0032123.
3. Berger S. 2010. Malaria: global status 2010 edition. Gideon Informatics, Inc, Los Angeles, CA.

4. Reference deleted.
5. Carme B, Demar M, Ajzenberg D, Dardé ML. 2009. Severe acquired toxoplasmosis caused by wild cycle of Toxoplasma gondii, French Guiana. Emerg Infect Dis 15:656–658. https://doi.org/10.3201/eid1504.081306.
6. Kemp LE, Yamamoto M, Soldati-Favre D. 2013. Subversion of host cellular functions by the apicomplexan parasites. FEMS Microbiol Rev 37:607–631. https://doi.org/10.1111/1574-6976.12013.
7. Carlson-Bremer D, Colegrove KM, Gulland FM, Conrad PA, Mazet JA, Johnson CK. 2015. Epidemiology and pathology of Toxoplasma gondii in free-ranging California sea lions (Zalophus californianus). J Wildl Dis 51:362–373. https://doi.org/10.7589/2014-08-205.
8. Innes EA. 2010. A brief history and overview of Toxoplasma gondii. Zoonoses Public Health 57:1–7. https://doi.org/10.1111/j.1863-2378.2009.01276.x.
9. Boothroyd JC. 2009. Expansion of host range as a driving force in the evolution of Toxoplasma. Mem Inst Oswaldo Cruz 104:179–184. https://doi.org/10.1590/s0074-02762009000200009.
10. Silva RC, Machado GP. 2016. Canine neosporosis: perspectives on pathogenesis and management. Vet Med (Auckl) 7:59–70. https://doi.org/10.2147/VMRR.S76969.
11. Dubey JP, Buxton D, Wouda W. 2006. Pathogenesis of bovine neosporosis. J Comp Pathol 134:267–289. https://doi.org/10.1016/j.jcpa.2005.11.004.
12. González-Warleta M, Castro-Hermida JA, Calvo C, Pérez V, Gutiérrez-Expósito D, Regidor-Cerrillo J, Ortega-Mora LM, Mezo M. 2018. Endogenous transplacental transmission of Neospora caninum during successive pregnancies across three generations of naturally infected sheep. Vet Res 49:106. https://doi.org/10.1186/s13567-018-0601-3.
13. Dubey JP, Carpenter JL, Speer CA, Topper MJ, Uggla A. 1988. Newly recognized fatal protozoan disease of dogs. J Am Vet Med Assoc 192:1269–1285.
14. Besteiro S, Dubremetz JF, Lebrun M. 2011. The moving junction of apicomplexan parasites: a key structure for invasion. Cell Microbiol 13:797–805. https://doi.org/10.1111/j.1462-5822.2011.01597.x.
15. Reid AJ, Vermont SJ, Cotton JA, Harris D, Hill-Cawthorne GA, Konen-Waisman S, Latham SM, Mourier T, Norton R, Quail MA, Sanders M, Shanmugam D, Sohal A, Wasmuth JD, Brunk B, Grigg ME, Howard JC, Parkinson J, Roos DS, Trees AJ, Berriman M, Pain A, Wastling JM. 2012. Comparative genomics of the apicomplexan parasites Toxoplasma gondii and Neospora caninum: coccidia differing in host range and transmission strategy. PLoS Pathog 8:e1002567. https://doi.org/10.1371/journal.ppat.1002567.
16. Williams DJ, Trees AJ. 2006. Protecting babies: vaccine strategies to prevent foetopathy in Neospora caninum-infected cattle. Parasite Immunol 28:61–67. https://doi.org/10.1111/j.1365-3024.2005.00809.x.
17. Esteban-Redondo I, Innes EA. 1997. Toxoplasma gondii infection in sheep and cattle. Comp Immunol Microbiol Infect Dis 20:191–196. https://doi.org/10.1016/s0147-9571(96)00039-2.
18. Nunes ACBT, da Silva EMV, de Oliveira JA, Yamasaki EM, Kim PDCP, de Almeida JC, Nunes KB, Mota RA. 2015. Application of different techniques to detect Toxoplasma gondii in slaughtered sheep for human consumption. Rev Bras Parasitol Vet 24:416–421. https://doi.org/10.1590/s1984-29612015076.
19. Dubey JP, Hill DE, Jones JL, Hightower AW, Kirkland E, Roberts JM, Marcet PL, Lehmann T, Vianna MCB, Miska K, Sreekumar C, Kwok OCH, Shen SK, Gamble HR. 2005. Prevalence of viable Toxoplasma gondii in beef, chicken, and pork from retail meat stores in the United States: risk assessment to consumers. J Parasitol 91:1082–1093. https://doi.org/10.1645/GE-683.1.
20. Dubey JP, Van Why K, Verma SK, Choudhary S, Kwok OC, Khan A, Behinke MS, Sibley LD, Ferreira LR, Oliveira S, Weaver M, Stewart R, Su C. 2014. Genotyping Toxoplasma gondii from wildlife in Pennsylvania and identification of natural recombinants virulent to mice. Vet Parasitol 200:74–84. https://doi.org/10.1016/j.vetpar.2013.11.001.
21. Gazzinelli RT, Wysocka M, Hayashi S, Denkers EY, Hieny S, Caspar P, Trinchieri G, Sher A. 1994. Parasite-induced IL-12 stimulates early IFN-gamma synthesis and resistance during acute infection with Toxoplasma gondii. J Immunol 153:2533–2543.
22. Suzuki Y, Orellana MA, Schreiber RD, Remington JS. 1988. Interferon-gamma: the major mediator of resistance against Toxoplasma gondii. Science 240:516–518. https://doi.org/10.1126/science.3128869.
23. Yarovinsky F. 2014. Innate immunity to Toxoplasma gondii infection. Nat Rev Immunol 14:109–121. https://doi.org/10.1038/nri3598.
24. Suzuki Y, Sher A, Yap G, Park D, Neyer LE, Liesenfeld O, Fort M, Kang H, Gufwoli E. 2000. IL-10 is required for prevention of necrosis in the small intestine and mortality in both genetically resistant BALB/c and susceptible C57BL/6 mice following peroral infection with Toxoplasma gondii. J Immunol 164:5375–5382. https://doi.org/10.4049/jimmunol.164.10.5375.
25. Khan A, Taylor S, Ajioka JW, Rosenthal BM, Sibley LD. 2009. Selection at a single locus leads to widespread expansion of Toxoplasma gondii lineages that are virulent in mice. PLoS Genet 5:e1000404. https://doi.org/10.1371/journal.pgen.1000404.
26. Saeij JP, Boyle JP, Grigg ME, Arrizabalaga G, Boothroyd JC. 2005. Bioluminescence imaging of Toxoplasma gondii infection in living mice reveals dramatic differences between strains. Infect Immun 73:695–702. https://doi.org/10.1128/IAI.73.2.695-702.2005.
27. Reese ML, Zeiner GM, Saeij JPJ, Boothroyd JC, Boyle JP. 2011. Polymorphic family of injected pseudokinases is paramount in Toxoplasma virulence. Proc Natl Acad Sci U S A 108:9625–9630. https://doi.org/10.1073/pnas.1015980108.
28. Dubey JP, Schares G, Ortega-Mora LM. 2007. Epidemiology and control of neosporosis and Neospora caninum. Clin Microbiol Rev 20:323–367. https://doi.org/10.1128/CMR.00031-06.
29. Mols-Vorstermans T, Hemphill A, Monney T, Schaap D, Boerhout E. 2013. Differential effects on survival, humoral immune responses and brain lesions in inbred BALB/C, CBA/CA, and C57BL/6 mice experimentally infected with Neospora caninum tachyzoites. ISRN Parasitol 2013:830980. https://doi.org/10.5402/2013/830980.
30. Aguado-Martínez A, Basto AP, Leitão A, Hemphill A. 2017. Neospora caninum in non-pregnant and pregnant mouse models: cross-talk between infection and immunity. Int J Parasitol 47:723–735. https://doi.org/10.1016/j.ijpara.2017.09.001.
31. Baszler TV, Long MT, McElwain TF, Mathison BA. 1999. Interferon-gamma and interleukin-12 mediate protection to acute Neospora caninum infection in BALB/c mice. Int J Parasitol 29:1635–1646. https://doi.org/10.1016/s0020-7519(99)00141-1.
32. Khan IA, Schwartzman JD, Fonseka S, Kasper LH. 1997. Neospora caninum: role for immune cytokines in host immunity. Exp Parasitol 85:24–34. https://doi.org/10.1006/expr.1996.4110.
33. Innes EA, Panton WRM, Marks J, Trees AJ, Holmdahl J, Buxton D. 1995. Interferon gamma inhibits the intracellular multiplication of Neospora caninum, as shown by incorporation of 3H uracil. J Comp Pathol 113:95–100. https://doi.org/10.1016/S0021-9975(05)80075-1.
34. Correia A, Ferreirinha P, Botelho S, Belinha A, Leitão C, Caramalho Í, Teixeira L, González-Fernandéz Á, Appelberg R, Vilanova M. 2015. Predominant role of interferon-γ in the host protective effect of CD8+ T cells against Neospora caninum infection. Sci Rep 5:14913. https://doi.org/10.1038/srep14913.
35. López-Gatius F, Almería S, Donofrio G, Nogareda C, García-Ispierto I, Bech-Sàbat G, Santolaria P, Yániz JL, Pabón M, de Sousa NM, Beckers JF. 2007. Protection against abortion linked to gamma interferon production in pregnant dairy cows naturally infected with Neospora caninum. Theriogenology 68:1067–1073. https://doi.org/10.1016/j.theriogenology.2007.08.006.
36. Maley SW, Buxton D, Macaldowie CN, Anderson IE, Wright SE, Bartley PM, Esteban-Redondo I, Hamilton CM, Storset AK, Innes EA. 2006. Characterization of the immune response in the placenta of cattle experimentally infected with Neospora caninum in early gestation. J Comp Pathol 135:130–141. https://doi.org/10.1016/j.jcpa.2006.07.001.
37. Gazzinelli RT, Mendonca-Neto R, Lilue J, Howard J, Sher A. 2014. Innate resistance against Toxoplasma gondii: an evolutionary tale of mice, cats, and men. Cell Host Microbe 15:132–138. https://doi.org/10.1016/j.chom.2014.01.004.
38. Schroder K, Hertzog PJ, Ravasi T, Hume DA. 2004. Interferon-gamma: an overview of signals, mechanisms and functions. J Leukoc Biol 75:163–189. https://doi.org/10.1189/jlb.0603252.
39. Saeij JP, Boyle JP, Coller S, Taylor S, Sibley LD, Brooke-Powell ET, Ajioka JW, Boothroyd JC. 2006. Polymorphic secreted kinases are key virulence factors in toxoplasmosis. Science 314:1780–1783. https://doi.org/10.1126/science.1133690.
40. Hemphill A, Aguado-Martínez A, Müller J. 2016. Approaches for the vaccination and treatment of Neospora caninum infections in mice and ruminant models. Parasitology 143:245–259. https://doi.org/10.1017/S0031182015001596.
41. Horcajo P, Regidor-Cerrillo J, Aguado-Martínez A, Hemphill A, Ortega-Mora LM. 2016. Vaccines for bovine neosporosis: current status and key aspects for development. Parasite Immunol 38:709–723. https://doi.org/10.1111/pim.12342.

42. Miller JL, Murray S, Vaughan AM, Harupa A, Sack B, Baldwin M, Crispe IN, Kappe SHI. 2013. Quantitative bioluminescent imaging of pre-erythrocytic malaria parasite infection using luciferase-expressing Plasmodium yoelii. PLoS One 8:e60820. https://doi.org/10.1371/journal.pone.0060820.
43. Dellacasa-Lindberg I, Hitziger N, Barragan A. 2007. Localized recrudescence of Toxoplasma infections in the central nervous system of immunocompromised mice assessed by in vivo bioluminescence imaging. Microbes Infect 9:1291–1298. https://doi.org/10.1016/j.micinf.2007.06.003.
44. Subauste C. 2012. Animal models for Toxoplasma gondii infection. Curr Protoc Immunol Chapter19:Unit 19.31-23. https://doi.org/10.1002/0471142735.im1903s96.
45. Grigg ME, Bonnefoy S, Hehl AB, Suzuki Y, Boothroyd JC. 2001. Success and virulence in *Toxoplasma* as the result of sexual recombination between two distinct ancestries. Science 294:161–165. https://doi.org/10.1126/science.1061888.
46. Goodswen SJ, Kennedy PJ, Ellis JT. 2013. A review of the infection, genetics, and evolution of Neospora caninum: from the past to the present. Infect Genet Evol 13:133–150. https://doi.org/10.1016/j.meegid.2012.08.012.
47. Sibley LD, Boothroyd JC. 1992. Construction of a molecular karyotype for Toxoplasma gondii. Mol Biochem Parasitol 51:291–300. https://doi.org/10.1016/0166-6851(92)90079-y.
48. Sibley LD, LeBlanc AJ, Pfefferkorn ER, Boothroyd JC. 1992. Generation of a restriction fragment length polymorphism linkage map for Toxoplasma gondii. Genetics 132:1003–1015.
49. Ellis J, Sinclair D, Morrison D, Al-Qassab S, Springett K, Ivens A. 2010. Microarray analyses of mouse responses to infection by Neospora caninum identifies disease associated cellular pathways in the host response. Mol Biochem Parasitol 174:117–127. https://doi.org/10.1016/j.molbiopara.2010.08.007.
50. Nishikawa Y, Tragoolpua K, Inoue N, Makala L, Nagasawa H, Otsuka H, Mikami T. 2001. In the absence of endogenous gamma interferon, mice acutely infected with Neospora caninum succumb to a lethal immune response characterized by inactivation of peritoneal macrophages. Clin Diagn Lab Immunol 8:811–816. https://doi.org/10.1128/CDLI.8.4.811-817.2001.
51. Mineo TW, Benevides L, Silva NM, Silva JS. 2009. Myeloid differentiation factor 88 is required for resistance to Neospora caninum infection. Vet Res 40:32. https://doi.org/10.1051/vetres/2009015.
52. Robben PM, LaRegina M, Kuziel WA, Sibley LD. 2005. Recruitment of Gr-1$^+$ monocytes is essential for control of acute toxoplasmosis. J Exp Med 201:1761–1769. https://doi.org/10.1084/jem.20050054.
53. Scanga CA, Aliberti J, Jankovic D, Tilloy F, Bennouna S, Denkers EY, Medzhitov R, Sher A. 2002. Cutting edge: MyD88 is required for resistance to Toxoplasma gondii infection and regulates parasite-induced IL-12 production by dendritic cells. J Immunol 168:5997–6001. https://doi.org/10.4049/jimmunol.168.12.5997.
54. Denkers EY. 2010. Toll-like receptor initiated host defense against Toxoplasma gondii. J Biomed Biotechnol 2010:737125. https://doi.org/10.1155/2010/737125.
55. Beiting DP, Peixoto L, Akopyants NS, Beverley SM, Wherry EJ, Christian DA, Hunter CA, Brodsky IE, Roos DS. 2014. Differential induction of TLR3-dependent innate immune signaling by closely related parasite species. PLoS One 9:e88398. https://doi.org/10.1371/journal.pone.0088398.
56. Miranda VDS, Franca FBF, da Costa MS, Silva VRS, Mota CM, Barros PDSC, Parreira KS, Santiago FM, Mineo JR, Mineo TWP. 2019. Toll-like receptor 3-TRIF pathway activation by Neospora caninum RNA enhances infection control in mice. Infect Immun 87:e00739-18. https://doi.org/10.1128/IAI.00739-18.
57. Yarovinsky F, Zhang D, Andersen JF, Bannenberg GL, Serhan CN, Hayden MS, Hieny S, Sutterwala FS, Flavell RA, Ghosh S, Sher A. 2005. TLR11 activation of dendritic cells by a protozoan profilin-like protein. Science 308:1626–1629. https://doi.org/10.1126/science.1109893.
58. Plattner F, Yarovinsky F, Romero S, Didry D, Carlier M-F, Sher A, Soldati-Favre D. 2008. Toxoplasma profilin is essential for host cell invasion and TLR11-dependent induction of an interleukin-12 response. Cell Host Microbe 3:77–87. https://doi.org/10.1016/j.chom.2008.01.001.
59. Kucera K, Koblansky AA, Saunders LP, Frederick KB, De La Cruz EM, Ghosh S, Modis Y. 2010. Structure-based analysis of Toxoplasma gondii profilin: a parasite-specific motif is required for recognition by Toll-like receptor 11. J Mol Biol 403:616–629. https://doi.org/10.1016/j.jmb.2010.09.022.
60. Adomako-Ankomah Y, Wier GM, Borges AL, Wand HE, Boyle JP. 2014. Differential locus expansion distinguishes Toxoplasmatinae species and closely related strains of Toxoplasma gondii. mBio 5:e01003-13. https://doi.org/10.1128/mBio.01003-13.
61. Koblansky AA, Jankovic D, Oh H, Hieny S, Sungnak W, Mathur R, Hayden MS, Akira S, Sher A, Ghosh S. 2013. Recognition of profilin by Toll-like receptor 12 is critical for host resistance to Toxoplasma gondii. Immunity 38:119–130. https://doi.org/10.1016/j.immuni.2012.09.016.
62. Tosh KW, Mittereder L, Bonne-Annee S, Hieny S, Nutman TB, Singer SM, Sher A, Jankovic D. 2016. The IL-12 response of primary human dendritic cells and monocytes to Toxoplasma gondii is stimulated by phagocytosis of live parasites rather than host cell invasion. J Immunol 196:345–356. https://doi.org/10.4049/jimmunol.1501558.
63. Olle P, Bessieres MH, Malecaze F, Seguela JP. 1996. The evolution of ocular toxoplasmosis in anti-interferon gamma treated mice. Curr Eye Res 15:701–707. https://doi.org/10.3109/02713689609003451.
64. McCabe RE, Luft BJ, Remington JS. 1984. Effect of murine interferon gamma on murine toxoplasmosis. J Infect Dis 150:961–962. https://doi.org/10.1093/infdis/150.6.961.
65. Behnke MS, Khan A, Lauron EJ, Jimah JR, Wang Q, Tolia NH, Sibley LD. 2015. Rhoptry proteins ROP5 and ROP18 are major murine virulence factors in genetically divergent South American strains of Toxoplasma gondii. PLoS Genet 11:e1005434. https://doi.org/10.1371/journal.pgen.1005434.
66. Taylor S, Barragan A, Su C, Fux B, Fentress SJ, Tang K, Beatty WL, Hajj HE, Jerome M, Behnke MS, White M, Wootton JC, Sibley LD. 2006. A secreted serine-threonine kinase determines virulence in the eukaryotic pathogen Toxoplasma gondii. Science 314:1776–1780. https://doi.org/10.1126/science.1133643.
67. Olias P, Etheridge RD, Zhang Y, Holtzman MJ, Sibley LD. 2016. Toxoplasma effector recruits the Mi-2/NuRD complex to repress STAT1 transcription and block IFN-gamma-dependent gene expression. Cell Host Microbe 20:72–82. https://doi.org/10.1016/j.chom.2016.06.006.
68. Gay G, Braun L, Brenier-Pinchart MP, Vollaire J, Josserand V, Bertini RL, Varesano A, Touquet B, De Bock PJ, Coute Y, Tardieux I, Bougdour A, Hakimi MA. 2016. Toxoplasma gondii TgIST co-opts host chromatin repressors dampening STAT1-dependent gene regulation and IFN-gamma-mediated host defenses. J Exp Med 213:1779–1798. https://doi.org/10.1084/jem.20160340.
69. Tanaka T, Nagasawa H, Fujisaki K, Suzuki N, Mikami T. 2000. Growth-inhibitory effects of interferon-gamma on Neospora caninum in murine macrophages by a nitric oxide mechanism. Parasitol Res 86:768–771. https://doi.org/10.1007/s004360000242.
70. Tobin CM, Knoll LJ. 2012. A patatin-like protein protects Toxoplasma gondii from degradation in a nitric oxide-dependent manner. Infect Immun 80:55–61. https://doi.org/10.1128/IAI.05543-11.
71. Scharton-Kersten TM, Yap G, Magram J, Sher A. 1997. Inducible nitric oxide is essential for host control of persistent but not acute infection with the intracellular pathogen Toxoplasma gondii. J Exp Med 185:1261–1273. https://doi.org/10.1084/jem.185.7.1261.
72. Oppmann B, Lesley R, Blom B, Timans JC, Xu Y, Hunte B, Vega F, Yu N, Wang J, Singh K, Zonin F, Vaisberg E, Churakova T, Liu M, Gorman D, Wagner J, Zurawski S, Liu Y, Abrams JS, Moore KW, Rennick D, de Waal-Malefyt R, Hannum C, Bazan JF, Kastelein RA. 2000. Novel p19 protein engages IL-12p40 to form a cytokine, IL-23, with biological activities similar as well as distinct from IL-12. Immunity 13:715–725. https://doi.org/10.1016/S1074-7613(00)00070-4.
73. Raetz M, Kibardin A, Sturge CR, Pifer R, Li H, Burstein E, Ozato K, Larin S, Yarovinsky F. 2013. Cooperation of TLR12 and TLR11 in the IRF8-dependent IL-12 response to Toxoplasma gondii profilin. J Immunol 191:4818–4827. https://doi.org/10.4049/jimmunol.1301301.
74. Mansilla FC, Capozzo AV. 2017. Apicomplexan profilins in vaccine development applied to bovine neosporosis. Exp Parasitol 183:64–68. https://doi.org/10.1016/j.exppara.2017.10.009.
75. Mansilla FC, Quintana ME, Langellotti C, Wilda M, Martinez A, Fonzo A, Moore DP, Cardoso N, Capozzo AV. 2016. Immunization with Neospora caninum profilin induces limited protection and a regulatory T-cell response in mice. Exp Parasitol 160:1–10. https://doi.org/10.1016/j.exppara.2015.10.008.
76. Jenkins MC, Tuo W, Feng X, Cao L, Murphy C, Fetterer R. 2010. Neospora caninum: cloning and expression of a gene coding for cytokine-inducing profilin. Exp Parasitol 125:357–362. https://doi.org/10.1016/j.exppara.2010.03.001.
77. Teixeira L, Marques RM, Ferreirinha P, Bezerra F, Melo J, Moreira J, Pinto A, Correia A, Ferreira PG, Vilanova M. 2016. Enrichment of IFN-γ produc-

ing cells in different murine adipose tissue depots upon infection with an apicomplexan parasite. Sci Rep 6:23475. https://doi.org/10.1038/srep23475.
78. Sturge CR, Benson A, Raetz M, Wilhelm CL, Mirpuri J, Vitetta ES, Yarovinsky F. 2013. TLR-independent neutrophil-derived IFN-gamma is important for host resistance to intracellular pathogens. Proc Natl Acad Sci U S A 110:10711–10716. https://doi.org/10.1073/pnas.1307868110.
79. Kamau ET, Srinivasan AR, Brown MJ, Fair MG, Caraher EJ, Boyle JP. 2012. A focused small-molecule screen identifies 14 compounds with distinct effects on Toxoplasma gondii. Antimicrob Agents Chemother 56:5581–5590. https://doi.org/10.1128/AAC.00868-12.
80. National Institutes of Health. 2002. Public Health Service policy on humane care and use of laboratory animals. Office of Laboratory Animal Welfare, National Institutes of Health, Bethesda, MD.